

# NATIONAL ADVISORY COMMITTEE FOR AERONAUTICS

TECHNICAL NOTE 3068

COMPARISON OF MODEL AND FULL-SCALE SPIN RECOVERIES

OBTAINED BY USE OF ROCKETS

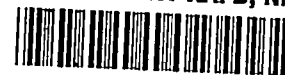
By Sanger M. Burk, Jr., and Frederick M. Healy

Langley Aeronautical Laboratory  
Langley Field, Va.



Washington  
February 1954

AFMEC  
TECHNICAL LIBRARY  
AFL 2811



## TECHNICAL NOTE 3068

## COMPARISON OF MODEL AND FULL-SCALE SPIN RECOVERIES

## OBTAINED BY USE OF ROCKETS

By Sanger M. Burk, Jr., and Frederick M. Healy

## SUMMARY

An investigation of a 1/19-scale model of an unswept-wing trainer airplane was conducted in the Langley 20-foot free-spinning tunnel to determine the rocket spin-recovery characteristics of the model for comparison with available full-scale-airplane results. A rocket was attached to each wing tip to fire in a direction to apply an antispin yawing moment about the Z body axis. The rockets were fired individually and in combination.

The results of the tests indicated that the recoveries of the model were in good agreement with those of the corresponding airplane, and for the design and loading tested, wing-tip rockets quickly terminated the spin. For the spins obtained, left- or right-wing-tip rockets appeared to be equally effective for recoveries.

## INTRODUCTION

Military airplanes generally are required to be spin demonstrated before they are accepted. During the spin demonstration, the airplane must be equipped with an emergency spin-recovery device in the event that the normal recovery technique (that is, by use of controls) is not successful. In the past, a spin-recovery parachute attached to the wing tip or tail has been used as an emergency device. Based on empirical results, a method for estimating the size of parachute required to effect a satisfactory recovery has been presented in reference 1. This method of estimating parachute size is based on the premise that the effectiveness of a parachute for spin recovery depends on its ability to provide a yawing moment opposing the spin. A serious disadvantage of parachutes is that the direction the towline assumes during the spin and recovery varies; therefore, only part of the parachute drag is available for producing a yawing moment. Another disadvantage is that, for some modern high-speed aircraft, the parachute size required to insure a recovery by parachute action alone has been excessively large so that heavy loads are

imposed on the airplane structure. In addition, the parachute characteristics usually must be demonstrated in normal flight prior to the spin tests and this testing of the parachute has in some instances been more expensive, dangerous, and time consuming than the actual spin program.

It therefore appears that a device that will provide a definite and direct yawing, pitching, or rolling moment, alone or in combination, to effect a recovery is desirable. The use of a rocket appears to be a desirable method of providing a definite known moment for emergency termination of the spin. The feasibility of such a device was indicated by previous spin-tunnel work (ref. 2) and it was felt that further evaluation of rockets as an emergency spin-recovery device should be made. Reference 3 presents results of an investigation conducted by North American Aviation, Inc., to evaluate the use of rockets on a full-scale airplane as an emergency device for recovery from spins. The airplane used for the tests was a current trainer design. A dynamic model of this airplane was built for the present investigation and tested in the Langley 20-foot free-spinning tunnel so that a direct comparison could be made between spin-tunnel and full-scale results of rocket recoveries. A rocket was attached to each wing tip to fire in a direction to apply an antispin yawing moment about the Z body axis.

#### SYMBOLS

An illustration of an airplane in a spin is shown in figure 1; the positive directions of the forces and moments along and about the body axes are also indicated.

X	longitudinal force acting along X body axis, positive forward, lb
Y	lateral force acting along Y body axis, positive to right, lb
Z	normal force acting along Z body axis, positive downward, lb
L	rolling moment acting about X body axis, positive when it tends to lower right wing, ft-lb
M	pitching moment acting about Y body axis, positive when it tends to increase angle of attack, ft-lb
N	yawing moment acting about Z body axis, positive when it tends to turn airplane to right, ft-lb
p	rolling angular velocity about X body axis, deg/sec

$q$	pitching angular velocity about Y body axis, deg/sec
$r$	yawing angular velocity about Z body axis, deg/sec
$\Omega$	angular velocity about spin axis, radians/sec unless otherwise indicated
$S$	wing area, sq ft
$b$	wing span, ft
$\rho$	air density, slugs/cu ft
$V$	rate of descent, ft/sec
$V_R$	resultant airspeed (resultant of the rate of descent of the airplane and the tangential velocity $\Omega R_S$ ) as measured by a swivel airspeed head mounted on a wing-tip boom, knots
$R_S$	spin radius, full-scale distance from spin axis to center of gravity, ft
$c$	local chord, ft unless otherwise indicated
$\bar{c}$	mean aerodynamic chord, ft unless otherwise indicated
$x/\bar{c}$	ratio of distance of center of gravity rearward of leading edge of mean aerodynamic chord to mean aerodynamic chord
$z/\bar{c}$	ratio of perpendicular distance between center of gravity and thrust line to mean aerodynamic chord (positive when center of gravity is below thrust line)
$W$	weight of airplane, lb
$g$	acceleration due to gravity, taken as 32.2 ft/sec <sup>2</sup>
$m$	mass of airplane, $W/g$ , slugs
$\mu$	airplane relative-density coefficient, $m/\rho S b$
$I_X, I_Y, I_Z$	moments of inertia about X, Y, and Z body axes, respectively, slug-ft <sup>2</sup>
$\frac{I_X - I_Y}{mb^2}$	inertia yawing-moment parameter

$\frac{I_Y - I_Z}{mb^2}$	inertia rolling-moment parameter
$\frac{I_Z - I_X}{mb^2}$	inertia pitching-moment parameter
$\alpha$	angle of attack (angle between projection of relative wind into plane of symmetry and X body axis), deg
$\theta_A$	angle of pitch (angle between X body axis and the horizontal) as measured by an attitude gyroscope, deg
$\theta_R$	angle of pitch (angle between the X body axis and the horizontal) as measured by a Reeves gyroscope, deg
$\phi$	angle of wing tilt (commonly called angle of bank; angle between span axis and the horizontal), positive when right wing is down, deg
$\phi_A$	angle of bank as measured by an attitude gyroscope, deg
$\phi_R$	angle of bank as measured by a Reeves gyroscope, deg
$\beta$	angle of sideslip, deg
$\eta$	compass direction, deg
$h$	altitude, ft
$T$	thrust of rocket, lb unless otherwise indicated
$t$	time, sec
$\delta_r$	rudder deflection with respect to chord line of fin, deg
$\delta_e$	elevator deflection with respect to chord line of stabilizer, deg
$\delta_a$	aileron deflection with respect to chord line of wing, deg

## Subscripts:

FS	full-scale airplane
M	model

## APPARATUS

## Full-Scale Airplane and Instrumentation

The airplane used in the investigation was an unswept-wing trainer. The data recorded on an oscillograph mounted in the airplane were obtained with the following instrumentation (see ref. 3):

(1) Pressure transducers to measure the airspeed and altitude were mounted near the root of a wing-tip boom. The static holes were located approximately 79 inches ahead of the leading edge of the wing. The swivel airspeed head was capable of alinement into the airstream direction through an angle-of-attack range of  $-5^{\circ}$  to  $85^{\circ}$  and through an angle-of-yaw range of  $\pm 45^{\circ}$ .

(2) Potentiometer-type instruments built by North American Aviation, Inc., were used to indicate separately the rudder, elevator, and aileron positions.

(3) Two Reeves gyroscopes to measure pitch and bank angles were mounted in the airplane. The axis of rotation of one gyroscope was perpendicular to the X airplane axis and the axis of rotation of the second gyroscope was tilted forward  $45^{\circ}$  with respect to the X airplane axis.

The data recorded on a photo recorder which was mounted in the airplane were obtained with the following instrumentation (see ref. 3):

(1) A clock was used to measure time.

(2) An attitude gyroscope was used to measure the angles of pitch and bank.

(3) Rate instruments were used to measure separately the rolling, pitching, and yawing angular velocities. However, for reasons unknown, the pitching-angular-velocity data were not presented in reference 3. The sense of the full-scale yawing angular velocity has been interpreted in terms of NACA conventions and consequently negative values have been interpreted as positive values.

(4) Angle-of-attack and angle-of-yaw vanes were installed on the end of the left- and right-wing-tip booms. The angle-of-attack range was from  $120^{\circ}$  to  $-60^{\circ}$ , and the angle-of-yaw range was  $\pm 90^{\circ}$ . As plotted, the full-scale angle-of-yaw data have been assumed to indicate sideslip rather than yaw.

(5) A compass was mounted on the wing tip and could be read remotely.

(6) Stall-warning lights were mounted on the photo-recorder panel. Safe-flight indicators were installed on each wing and connected to the warning lights which illuminated when either wing was in the stalled condition; these indicators had previously been calibrated in level-flight stalls.

(7) Lights indicating full control-surface displacement were mounted on the photo-recorder panel. A separate light for the ailerons, elevator, and rudder illuminated when each control surface was at its full displacement.

### Model

A 1/19-scale model of the airplane was constructed at the Langley Laboratory. The model was made almost entirely of plastic. A three-view drawing of the model with the rockets installed at the wing tips is shown in figure 2. A photograph of the model is presented as figure 3. The dimensional characteristics of the airplane represented by the model are shown in table I.

### Model Rocket

The rockets used for the dynamic model tests were designed by the Langley Model Propulsion Section of the Pilotless Aircraft Research Division. The rockets are precision built and made of steel. Photographs of the rockets installed on the wing tips of the model are shown as figures 3 and 4. A diagrammatic sketch of one of the rockets and the electrical circuit is shown in figure 5.

The rocket consists of two chambers set at right angles to each other. The small chamber contains the igniter which is set off when current flows through a high-resistance wire embedded in it. The flame from the igniter strikes the end of the main propellant or grain (solid cordite) in the large chamber and causes it to burn; this burning provides the actual thrust. The grain is partly encased in a nonburning substance (inhibitor) so that the propellant will have a constant burning area. The only exposed part of the propellant is the end where it is ignited. The grain is machined very accurately so as to give the required thrust for the required time as closely as possible.

The magnitude and duration of the rocket thrust for several rockets are shown in figure 6. These curves were obtained by discharging the rocket mounted on a strain-gage balance and recording the data on an oscillograph. It should be noted that the impulses are very similar and the magnitude and time of the rocket firings are fairly similar. The rockets were designed to provide approximately 3 ounces of thrust for

2.0 seconds. Although the rockets were not scaled down intentionally in regard to size and weight, they nevertheless did simulate approximately the full-scale rockets in these respects.

## METHODS

### Wind Tunnel and Testing Technique

The model tests were performed in the Langley 20-foot free-spinning tunnel, the operation of which is generally similar to that of the Langley 15-foot free-spinning tunnel which is described in reference 4, except that the model launching technique has been changed. With the controls set in the desired position, the model is now launched by hand with rotation into the vertically rising airstream. After a number of turns in the established spin, recovery is normally attempted by moving one or more controls by means of a remote-control mechanism installed in the model. After recovery the model dives into a safety net. For the current investigation, the remote-control mechanism was generally used only to activate the rocket or to reverse the rudder.

In order to determine the spin and recovery characteristics of the model corresponding to a loading condition of the airplane for which rockets were installed, tests were performed for the normal spinning control configuration (elevator full up, ailerons neutral, and rudder full with the spin) and for various other aileron-elevator combinations including neutral and maximum settings of the surfaces. Recovery was generally attempted by rapid reversal of the rudder from full with to full against the spin. A few tests were also performed to evaluate the possible adverse effects on recovery of small deviations from the normal control configuration for spinning. For these tests, the elevator was set at either full up or two-thirds of its full-up deflection and the ailerons were set at one-third of full deflection in the direction conducive to slower recoveries, ailerons with the spin for the loading tested on this model. (Ailerons deflected with the spin means that a stick-right condition in a right spin was simulated.) Recovery from this spin was attempted by rapidly reversing the rudder from full with to only two-thirds against the spin or by simultaneous rudder reversal to two-thirds against the spin and movement of the elevator to one-half of full down deflection. These control configurations and manipulations are referred to as the "criterion spin."

Turns for recovery are measured from the time the controls are moved, or the rocket is fired, to the time the spin rotation ceases. For recovery attempts in which the model struck the safety net while it was still in a spin, the turns for recovery were recorded as greater than the number of turns from the time the controls were moved to the time the model struck



the net, for example >3. A >3-turn recovery, however, does not necessarily indicate an improvement over a >7-turn recovery. When the model recovered without control movement (rudder with the spin), the results were recorded as "no spin." Recovery characteristics were considered satisfactory if recovery from the spin occurred in  $2\frac{1}{4}$  turns or less.

This criterion was used on the basis of a correlation of available full-scale-airplane spin-recovery data and corresponding model test results.

For the model rocket spin-recovery tests, the controls were maintained with the spin (i.e., rudder with the spin, elevator up, and ailerons with the spin) and the rocket was fired so as to apply an anti-spin yawing moment. The recovery was thus due entirely to the action of the rocket. Each test generally was made at least three times as a check on the results.

Motion pictures normally are taken only from the side of the tunnel on a level with the spinning model to record its motion. However, for the present investigation, in order to locate the spin axis relative to the model, motion pictures also were taken with a camera placed in the center of the bottom of the tunnel, just below the safety net.

#### Conversion of Data

The results of the model tests have been converted to corresponding full-scale values by methods described in reference 4.

The average rate of descent of the actual full-scale airplane during the developed spin was determined by taking the average slope of a plot of altitude against time. The turns for recovery of the airplane were determined from a photographic time history of the compass direction. The instantaneous angular velocity about the spin axis of the airplane as presented in reference 3 was calculated by the following formula:

$$\Omega = \sqrt{p^2 + q^2 + r^2}$$

although  $q$  was assumed to be zero.

## TEST CONDITIONS

## Full-Scale Airplane

All full-scale spin tests were performed with the rockets fully loaded. Spin recoveries of the airplane generally were initiated at altitudes ranging from 14,000 to 18,000 feet. The mass characteristics and inertia parameters of the airplane and model are listed in table II. The inertia parameters for the loadings tested on the airplane and for the loading tested on the model are shown in figure 7. The control settings and the locations of the rockets for the various full-scale tests are presented in table III. The control deflections varied slightly for different spins probably because the pilot had difficulty in maintaining the exact setting each time.

Rockets were mounted on both the left and right wing tips of the airplane to determine the relative effectiveness of applying a yawing moment about the Z body axis as compared to the spin axis. Inasmuch as the spin axis may be to the right or left of the plane of symmetry, the moment arms of the right- and left-wing-tip rockets in such a case will be unequal; thus the yawing moment applied by one rocket will be greater than that applied by the other. However, inasmuch as the Z body axis lies in the plane of symmetry, the yawing moments about this axis will be equal.

On each wing tip, two positions of the rockets were tested during the full-scale spin tests. For one position, the rockets were installed at the wing tips where a small amount of pitching moment was applied to the airplane when one rocket was fired because the thrust of the rocket was 11 inches above the airplane center of gravity. In order to eliminate this pitching moment and thus to determine the effect of pure yawing moment applied about the airplane center of gravity, an alternate rocket mount 11 inches below the wing tip was also tested.

For the full-scale spin tests, commercial jato bottles were used which were rated at 800 pounds of thrust for a duration of about 8 seconds.

## Model

It was originally decided to ballast the model to obtain dynamic similarity to the airplane at an altitude of 15,000 feet ( $\rho = 0.001496$  slug/cu ft). On this assumption the model rockets were built to provide 3 ounces of thrust which for 1/19 scale would be equivalent to full-scale thrust of 800 pounds. Because of weight considerations, however, the model had to be ballasted at a simulated altitude of 20,000 feet. Although the actual thrust of the model rocket remained the same, the corresponding full-scale value at the higher altitude was

accordingly reduced from 800 pounds to approximately 700 pounds of thrust (altitude of 20,000 feet;  $\rho = 0.001267$  slug/cu ft). As previously mentioned, the mass characteristics and inertia parameters of the model are presented in table II. The control settings used during the model spin tests are presented in table IV.

The two rocket locations tested on the airplane were tested briefly on the model to determine whether any aerodynamic effects were present. With the rockets installed at the wing tips (fig. 2), the steady-spin and recovery characteristics of the model by rudder reversal were noted. Then flat lead weights (same weight as rockets) were substituted for the rockets at the wing tips and the steady-spin and recovery characteristics again noted. Next the model was properly ballasted with lead weights substituted for the rockets, and dummy balsa rockets (weight negligible) were placed below the wing tips (fig. 8) and the steady-spin and recovery characteristics noted.

### PRECISION

The limits of accuracy of the full-scale data are not known. These limits would depend on the accuracy of the flight instruments.

### Model

The spin-tunnel results presented herein are believed to be the true values for the model within the following limits:

$\alpha$ , deg . . . . .	$\pm 1$
$\phi$ , deg . . . . .	$\pm 1$
V, percent . . . . .	$\pm 5$
$\Omega$ , percent . . . . .	$\pm 2$
Turns for recovery:	
When obtained from motion-picture records . . . . .	$\pm 1/4$
When obtained by visual estimate . . . . .	$\pm 1/2$

Comparison between model and full-scale results in reference 5 indicated that model tests satisfactorily predicted full-scale recovery characteristics approximately 90 percent of the time and that, for the remaining 10 percent of the time, the model results were of value in predicting some of the details of the full-scale spins. The airplanes generally spun at an angle of attack closer to  $45^\circ$  than did the corresponding models. The comparison presented in reference 5 also indicated that generally the airplane spun with the inner wing tilted more downward and with a greater altitude loss per revolution than did the corresponding model,

although the higher rate of descent was found to be generally associated with the smaller angle of attack regardless of whether it was for the model or the airplane.

Because it is impracticable to ballast the model exactly and because of inadvertent damage to the model during tests, the measured weight and mass distribution of the model varied from the true scaled-down values within the following limits:

Weight, percent . . . . . 1 high to 2 high  
 Center-of-gravity location, percent  $\bar{c}$  . . . . . 1 forward to 0 rearward  
 Moments of inertia:  
 $I_x$ , percent . . . . . 5 low to 7 high  
 $I_y$ , percent . . . . . 5 low to 9 high  
 $I_z$ , percent . . . . . 3 high to 10 high

The accuracy of measuring the weight and mass distribution of the model is believed to be within the following limits:

Weight, percent . . . . .  $\pm 1$   
 Center-of-gravity location, percent  $\bar{c}$  . . . . .  $\pm 1$   
 Moments of inertia, percent . . . . .  $\pm 5$

Controls were set with an accuracy of  $\pm 1^\circ$ .

#### Model Rocket

The following values of the model-rocket thrust and impulse are considered to be representative of the values that were obtained during the rocket-firing tests:

Thrust, oz	Impulse, oz-sec
3.00 (desired value)	5.40 (desired value)
3.34	6.67
2.92	6.29
2.90	6.23

#### RESULTS AND DISCUSSION

The results of the full-scale and model tests are presented in table V, figures 9 to 14, and charts 1 and 2. The results, in general,

are presented in terms of right spins, the direction in which the airplane was spun. However, a few tests were performed with the model spinning to the left for comparison of left and right spins. Model results for left and right spins and recoveries by rudder reversal generally were similar (chart 1). The model data are presented in terms of full-scale values for the corresponding airplane at a test altitude of 20,000 feet. Spin tests, previously mentioned, performed on the model to determine if there were any aerodynamic effects due to the different locations of the rockets indicated no appreciable differences in the steady-spin characteristics or recoveries (chart 2). Consequently, because of greater ease of installation, all model rocket-firing tests were performed with the rockets located at the wing tips.

### Full-Scale Spin Recoveries by Rockets

The results of the full-scale rocket spin-recovery tests are presented in figures 9 to 14. In general, the motion of the airplane in the steady spin and recovery was fairly similar for all the spin tests. Although in a few cases the data were erratic, in general the airplane appeared to oscillate in roll, pitch, and yaw during the spin and recovery. Figures 9 to 12 present the results of tests for which rockets were fired individually on the left or right wing tip or on a lowered mount. For comparison purposes the time histories of the angular velocities of the airplane about the spin axis for all airplane flights have been plotted in figure 14.

Analysis of the results indicates, in general, that approximately 4 seconds after the rocket was fired, the rate of rotation of the airplane had decreased appreciably (fig. 14); the angle of attack of the outer wing tip decreased until it was well below the stall ( $\alpha = 20^\circ$ ); and the angle of attack of the inner wing tip, although still above the stall, had decreased appreciably. At this stage, analysis indicates that the airplane spin was terminated but because the controls were held in a pro-spin condition (rudder full with the spin, elevator full up, and ailerons full with the spin) the spin rotation began to build up rapidly to the right again and the airplane appeared to reenter a spin (figs. 9, 10, and 11). If the controls had been neutralized 4 seconds after the rocket was fired, the airplane probably would not have gone back into the spin. However, because the controls were held in a pro-spin condition and because they became very effective at the low angle of attack reached because of the rocket firing, the rudder tended to yaw the airplane back into the spin, the elevator tended to pitch the airplane back above the stall, and the ailerons forced the airplane to continue to rotate due to aileron roll. Thus the rate of rotation increased again and the angle of attack increased until it was again beyond the stall. The airplane continued to oscillate about all three axes until the end of the rocket-burning period (approximately 8 seconds) when again the same condition prevailed as that at the end of 4 seconds. The airplane again appeared

to be out of the spin, and if the controls were neutralized at this time, the airplane undoubtedly would not go back into the spin. However, the results in figures 9, 10, and 11 indicate that the controls were not neutralized quickly so that the rate of rotation again increased and the angle of attack again increased to beyond the stall. A few seconds later the controls were reversed and the airplane recovered from the spin.

For another test flight, the results of which are presented in figure 12, 4 seconds after the rocket was fired the airplane rotation was practically terminated by the rocket action alone even though the controls were held in a pro-spin direction. Although the airplane began to pitch up at the end of these 4 seconds, the spin rotation did not begin to build up again to the right until the rocket had just about burned out (8 seconds). The pilot moved the controls from their pro-spin settings immediately after the rocket burned out for this test and the airplane did not reenter a spin.

The results of firing left and right rockets simultaneously on lowered mounts are presented in figure 13. Approximately 3 seconds after the rockets were fired, the spin of the airplane was momentarily terminated. However, as a result of the excess rocket thrust the airplane went into a left spin from which recovery was effected by control movement.

In general, it appears that approximately 4 seconds after the right-hand rocket on the lowered mount was fired for two similar spin tests (figs. 9 and 10) the airplane was out of the spin in  $1\frac{1}{2}$  and 1 turn, respectively. When the left-hand rocket on either the lowered mount (fig. 11) or on the wing tip (fig. 12) was fired, it appears that the airplane was out of the spin at the end of 1 turn for both tests. When both left- and right-hand rockets were fired simultaneously, recovery was accomplished in about  $\frac{3}{4}$  turn. From these observations it would appear that spin recoveries were effected equally well by firing either the left- or right-hand rocket. Also, mounting the rocket directly at the wing tip or on a mount beneath the tip apparently had no appreciable effect on the recoveries.

#### Model Spin Recoveries by Rudder Reversal

Prior to determining the recovery characteristics of the model as effected by rockets, the recovery characteristics by use of the controls were determined. For these tests, the rockets were installed on the model but recoveries were attempted by rudder and elevator reversal.

For the normal control configuration (elevator full up, ailerons neutral, and rudder full with the spin) the model spun at an angle of

attack of approximately  $40^\circ$  and recovered satisfactorily in  $1\frac{1}{4}$  turns or less upon full rapid rudder reversal (chart 1). However, recoveries from the criterion spin (elevator two-thirds up and ailerons one-third with the spin) were unsatisfactory when the rudder was reversed from full with the spin to only two-thirds against the spin. When rudder reversal to two-thirds against the spin was accompanied by moving the elevator from two-thirds up to one-half below neutral, the model recovered satisfactorily in  $2\frac{1}{4}$  turns or less. When the elevator was neutral or down and the ailerons were against the spin, the model would not spin. Setting the ailerons from with to against the spin generally improved the recoveries. These results appear to be in general agreement with those of reference 6. When the ailerons were set with the spin, the model generally would rotate about its X body axis in the recovery dive because of aileron roll.

Before the rockets were fired, the developed spin characteristics of the model were obtained with the controls set in the same position as on the airplane when ready for rocket-firing tests (rudder with the spin, elevator up, and ailerons with the spin). These control settings, as previously mentioned, varied slightly from spin to spin because the pilot had difficulty in maintaining the exact settings. Therefore, the model control settings were varied in a like manner. The spin characteristics for these configurations of the model were noted and the results are compared with those for the airplane in table V. In spite of the slight difference in altitude between the model and the airplane and in spite of some scale effects between the model and the airplane, the values of the angle of attack and rate of rotation generally were in good agreement. The inner wing was down considerably less for the model than for the airplane; this difference may be attributed primarily to scale effect as indicated in reference 5. The higher rate of descent indicated from model tests may be primarily attributable to the higher wing loading associated with the model tests at the slightly higher altitude and the smaller angle of attack of the model.

#### Model Spin Recoveries by Rockets

With the rudder full with the spin, elevator full up, and ailerons full with the spin, model recovery tests were made to determine the effectiveness of the rockets. Turns for recovery are compared with those of the airplane in table V. When the left-wing-tip rocket was fired, thrust rearward (antispin yawing moment), recoveries generally were accomplished in  $\frac{1}{2}$  to  $1\frac{3}{4}$  turns. It would appear that the differences in types of recovery may be attributed to the phase of the oscillation in roll,

pitch, or yaw during which the rocket was fired or to some variation in rocket thrust, or both. When the right-wing-tip rocket was fired, thrust forward, recoveries generally were similar to those obtained by firing the left-wing-tip rocket ( $\frac{1}{2}$  to 1 turn). As in the case of recoveries by rudder reversal, the model generally continued to turn somewhat due to aileron roll. Recoveries generally were accomplished in about  $1/4$  turn when both right- and left-wing-tip rockets on the model were fired simultaneously. For these tests, the model sometimes continued to turn to the right during the recovery due to aileron roll; whereas at other times the model stopped spinning to the right and started spinning to the left.

As previously mentioned, for a single test on the airplane when both rockets were fired simultaneously, the airplane went from a right to a left spin. It is possible that, if several repeat tests had been made with the airplane, different types of recoveries similar to the model recoveries might have occurred.

A film strip showing the model recovering from a right spin and going into a left spin by firing both rockets simultaneously is presented in figure 15. It should be noted that the initial flash in the picture is the igniter firing which starts the rocket propellant burning. Although the rocket propellant then burns continuously throughout the rest of the film, it cannot be seen in the figure because the flame is very small.

From the analysis of the model results, it appears that for the spins obtained, spin recovery could be effected equally well by firing either the left- or right-wing-tip rocket. As previously mentioned, full-scale tests were made with right- and left-wing-tip rockets installed on the airplane in an attempt to ascertain the relative effectiveness of the application of a yawing moment about the Z body axis as compared to that about the spin axis. The full-scale results indicated approximately equal effectiveness of left- or right-wing-tip rockets although it was not readily apparent how to locate the airplane spin axis from the full-scale data. From film data obtained for the model with the camera at the bottom of the tunnel, it was indicated that the spin axis passed through the nose of the model and therefore each wing tip was equally distant from the spin axis. Thus these tests cannot be taken as an indication of the relative importance of application of a moment about the Z body axis or the spin axis.

In general, good agreement was obtained between the turns for recovery of the model and those of the full-scale airplane (table V). As previously mentioned, the airplane generally was out of the spin at the end of 4 seconds after the rocket was fired and then went back into the spin again because the controls were not neutralized. Similarly, the model recovered in the tunnel in approximately 4 seconds (full-scale)



after the rocket was fired; it then struck the safety net in a rolling dive with the rocket still burning. It is possible that, if sufficient height and airspeed were available in the tunnel, the model might have gone back into a spin in a manner similar to that of the airplane.

#### Mass Changes Associated With Installation of Emergency Device

In determining the spin and recovery characteristics of an airplane during a spin demonstration by use of controls alone, care should be taken that the emergency spin-recovery device, primarily because of its weight, does not change the inertia parameters of the airplane in such a manner as to mask its true spin and recovery characteristics. Probably the most important single inertia parameter is the inertia yawing-moment parameter (ref. 6). When the rockets are attached to the wing tips of the airplane, it is very possible, depending on the weight of the rockets and the original mass loading of the airplane, to change the inertia yawing-moment parameter from a negative value (mass distributed chiefly along fuselage) to a positive value (mass distributed chiefly along wings). Thus, although the airplane normally might recover by rudder reversal alone for negative loadings, it is possible it would not recover when the loading is positive unless the elevator is moved down (ref. 6). For the airplane used in the present investigation the addition of the rockets to the wing tips changed the inertia yawing-moment parameter from a value of  $-67 \times 10^{-4}$  to  $10 \times 10^{-4}$ .

The model spin results, as previously mentioned, indicated that for some control configurations the model would recover satisfactorily by rudder reversal alone even though the loading was positive. This recovery is possible because the airplane has a very high tail damping power factor. Reference 7 indicates that an airplane may have a positive loading and still recover by rudder reversal alone if the tail damping power factor is large enough. It is very possible, however, that if the tail damping power factor of this airplane had been lower it would not have recovered by rudder reversal alone. Therefore, for some airplanes where the addition of rockets to the wing tips may change the inertia yawing-moment parameter from a negative value to a positive value, the airplane may have to be ballasted to keep the original loading condition so that the true spin and recovery characteristics of the airplane can be determined.

#### CONCLUSIONS

Results of a spin-tunnel investigation of a dynamic model using wing-tip rockets as a spin-recovery device and a comparison of the results with corresponding full-scale results lead to the following conclusions:

1. The recoveries of the model were in good agreement with those of the corresponding airplane; for the design and loading tested, wing-tip rockets quickly terminated the spin.

2. Left- or right-wing-tip rockets appeared to be equally effective for recoveries for the spins obtained.

3. In determining the spin and recovery characteristics of an airplane by use of controls alone, cognizance should be taken of the fact that the emergency spin-recovery device, primarily because of its weight, may change the mass characteristics of the airplane in such a manner as to mask the true spin and recovery characteristics.

Langley Aeronautical Laboratory,  
National Advisory Committee for Aeronautics,  
Langley Field, Va., October 20, 1953.

## REFERENCES

1. Malvestuto, Frank S., Jr.: Method of Estimating the Minimum Size of a Tail or Wing-Tip Parachute for Emergency Spin Recovery of an Airplane. NACA RM 18D27, 1948.
2. Neihouse, Anshal I.: Spin-Tunnel Investigation To Determine the Effectiveness of a Rocket for Spin Recovery. NACA TN 1866, 1949.
3. Farmer, G. H., and Peterson, B. G.: Flight Test Investigation To Determine the Effectiveness of a Rocket as an Emergency Spin Recovery Device. Rep. No. NA-52-771 (Contract AF 33 (038)-23809), North American Aviation, Inc., June 27, 1952.
4. Zimmerman, C. H.: Preliminary Tests in the NACA Free-Spinning Wind Tunnel. NACA Rep. 557, 1936.
5. Berman, Theodore: Comparison of Model and Full-Scale Spin Test Results for 60 Airplane Designs. NACA TN 2134, 1950.
6. Neihouse, A. I.: A Mass-Distribution Criterion for Predicting the Effect of Control Manipulation on the Recovery From a Spin. NACA WR L-168, 1942. (Formerly NACA ARR, Aug. 1942.)
7. Neihouse, Anshal I., Lichtenstein, Jacob H., and Pepoon, Philip W.: Tail-Design Requirements for Satisfactory Spin Recovery. NACA TN 1045, 1946.

TABLE I.- DIMENSIONAL CHARACTERISTICS OF THE AIRPLANE REPRESENTED

BY THE 1/19-SCALE SPIN MODEL

Length, ft . . . . .	32.47
Wing:	
Span, ft . . . . .	40.6
Area, sq ft . . . . .	271.1
Root chord, in. . . . .	98.4
Tip chord, in. . . . .	61.37
$\bar{c}$ , in. . . . .	81.44
Leading edge of $\bar{c}$ rearward of leading edge of root chord, in. . . . .	1.14
Aspect ratio . . . . .	6.08
Taper ratio . . . . .	0.625
Dihedral, deg . . . . .	8
Incidence, deg	
Root . . . . .	2
Tip . . . . .	-1
Airfoil section . . . . .	NACA 64 <sub>2</sub> A215
Ailerons:	
Area, total, sq ft . . . . .	25.8
Span, percent b/2 . . . . .	36.74
Chord, percent c . . . . .	30
Horizontal tail:	
Span, ft . . . . .	16.4
Area, sq ft . . . . .	59.7
Root chord, in. . . . .	56.4
Tip chord, in. . . . .	31.62
Aspect ratio . . . . .	4.51
Elevator area, total, sq ft . . . . .	16.5
Elevator hinge line rearward of wing c/4, ft . . . . .	18.73
Dihedral, deg . . . . .	0
Incidence, deg . . . . .	1
Airfoil section . . . . .	NACA 64 <sub>1</sub> A012
Vertical tail:	
Fin area, sq ft . . . . .	18.2
Rudder area, sq ft . . . . .	12.1
Dorsal-fin area, sq ft . . . . .	4.32
Chord at fuselage intersection, in. . . . .	67.13
Tip chord, in. . . . .	35.75
Rudder span, ft . . . . .	8.61
Aspect ratio . . . . .	1.38
Rudder hinge line rearward of wing c/4, ft . . . . .	20.73
Fin offset, deg . . . . .	1 left
Airfoil section . . . . .	NACA 64 <sub>1</sub> A012
Tail damping power factor . . . . .	682 × 10 <sup>-6</sup>

TABLE II.- MASS CHARACTERISTICS AND INERTIA PARAMETERS FOR LOADINGS USED ON AIRPLANE

AND FOR LOADING TESTED ON THE 1/19-SCALE MODEL

[Model values are given as corresponding full-scale values; moments of inertia are given about center of gravity.]

Loading	Weight, lb	Center-of-gravity location		Relative density, $\mu$		Moments of inertia, slug-ft <sup>2</sup>			Mass parameters		
		$x/\bar{c}$	$z/\bar{c}$	Sea level	20,000 feet	$I_X$	$I_Y$	$I_Z$	$\frac{I_X - I_Y}{mb^2}$	$\frac{I_Y - I_Z}{mb^2}$	$\frac{I_Z - I_X}{mb^2}$
Airplane values											
1 (with rockets)	7,224	0.233	-0.110	8.57	16.08	9,207	8,833	17,149	$10 \times 10^{-4}$	$-225 \times 10^{-4}$	$215 \times 10^{-4}$
2 (without rockets)	6,998	.232	-.114	8.30	15.59	6,439	8,825	14,387	-67	-155	222
Model values											
1 (with rockets)	7,349	0.232	0.038	8.72	16.36	9,482	9,157	18,444	9	-247	238

TABLE III.- CONTROL SETTINGS, LOCATIONS OF ROCKETS, AND  
DIRECTIONS OF ROCKET THRUST FOR AIRPLANE TESTS

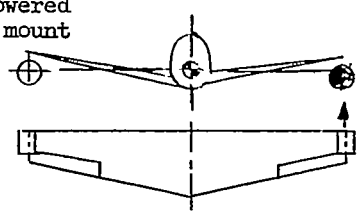
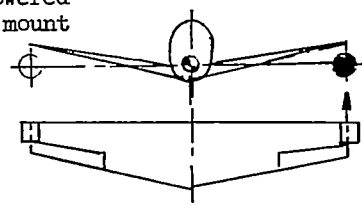
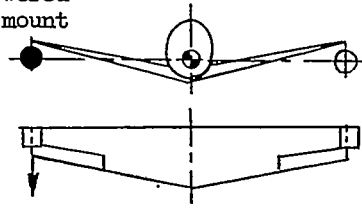
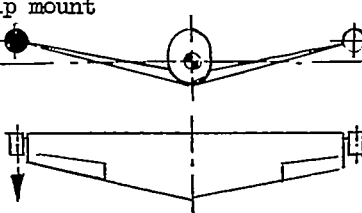
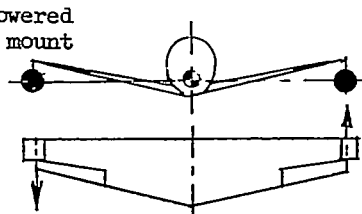
Rudder deflection, deg	Elevator deflection, deg	Aileron deflection, deg		Recovery attempted by use of rockets alone	Position of rockets
		Right	Left		
28 right	25 up	15.8 up	8.8 down	Right rocket fired, thrust forward	Lowered mount 
28 right	20 up	16 up	9 down	Right rocket fired, thrust forward	Lowered mount 
26.5 right	25 up	15.6 up	8.8 down	Left rocket fired, thrust rearward	Lowered mount 
26 right	25 up	16 up	9 down	Left rocket fired, thrust rearward	Tip mount 
31 right	20.5 up	16.2 up	9 down	Both right and left rockets fired simultaneously	Lowered mount 

TABLE IV.- RANGES OF CONTROL DEFLECTIONS USED FOR MODEL TESTS

Method of recovery	Range of rudder deflection, deg		Range of elevator deflection, deg		Range of aileron deflection, deg	
	Right	Left	Up	Down	Up	Down
Rudder reversal	25	25	26	10	16	9
Left- or right-wing-tip rocket fired	26	(a)	26	(a)	16	9
Left- and right-wing-tip rockets fired simultaneously	31	(a)	20	(a)	16	9

<sup>a</sup>Controls were held fixed when rockets were used for recovery.

TABLE V.- COMPARISON BETWEEN MODEL AND AIRPLANE SPIN  
AND RECOVERY CHARACTERISTICS

[Loading 1 in table II and figure 7; recovery attempted by firing rockets as indicated; right erect spins; control setting for spin is elevator full up, ailerons full with spin, rudder full with spin; control-setting values as indicated in table IV]

Location of rockets fired for recovery attempt	Test vehicle	$\alpha$ , deg	$\phi$ , deg (a)	V, ft/sec (b)	$\Omega$ , radians/sec (b)	Turns for recovery
Right wing tip	Model	48	3D	198	0.383	$\frac{c}{2}, \frac{c}{4}, \frac{c}{4}, c_1$
Below right wing tip	Airplane	58	14D	127	.383	$1\frac{1}{2}$
Below right wing tip (repeat test)	Airplane	57	28D	143	.389	1
Left wing tip	Model	48	3D	198	.383	$\frac{c}{2}, \frac{c}{4}, \frac{c}{4}$
Left wing tip	Airplane	55	18D	160	.386	1
Below left wing tip	Airplane	55	16D	143	.389	1
Both wing tips	Model	46	5D	198	.412	$\frac{d}{4}, \frac{d}{4}, \frac{d}{4}, \frac{c}{4}, \frac{c}{4}$
Below both wing tips	Airplane	56	22D	152	.384	$\frac{3}{4}$

<sup>a</sup>D inner wing down.

<sup>b</sup>Model values converted to corresponding full-scale values.

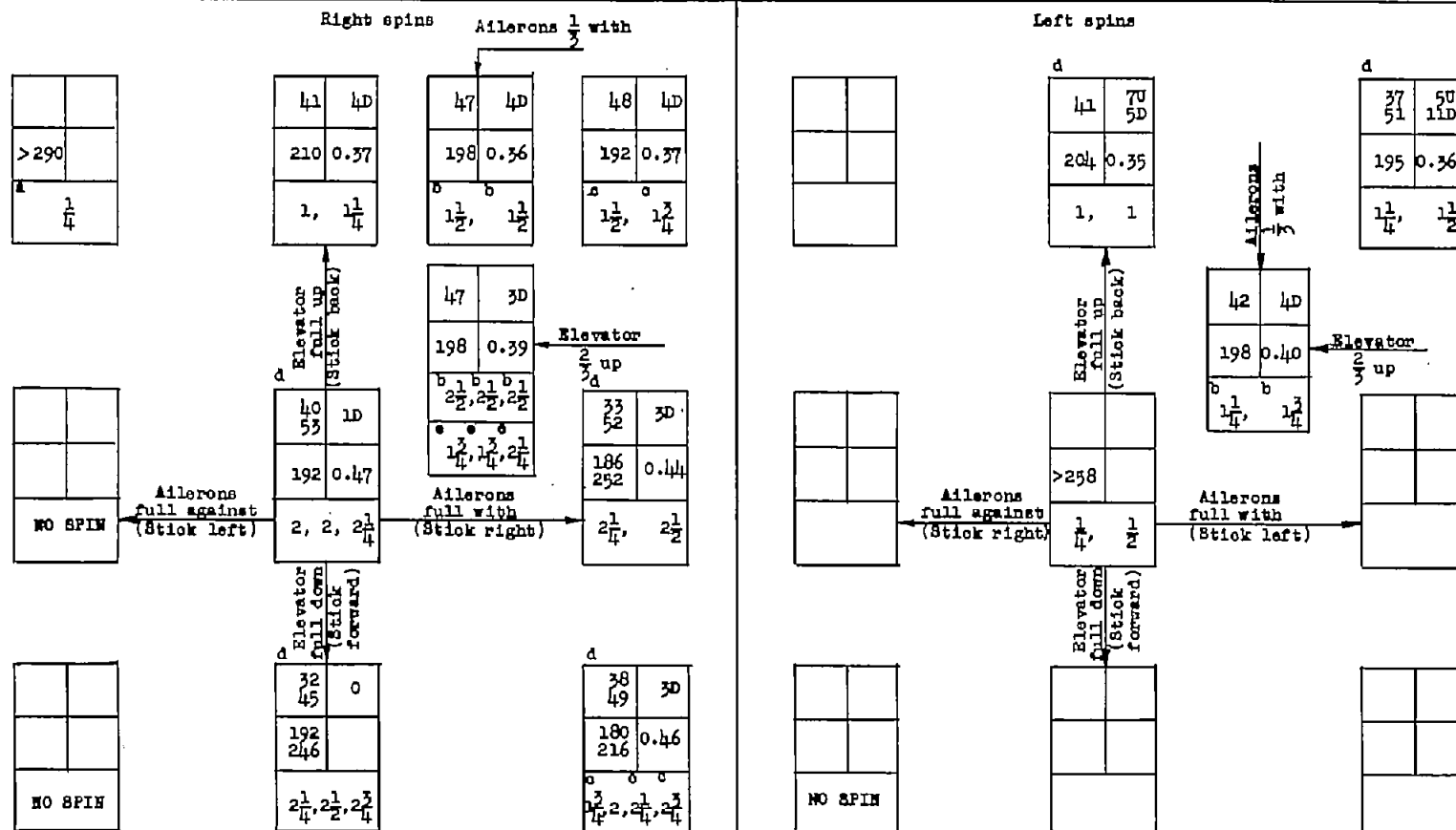
<sup>c</sup>Model entered into glide and then rolled.

<sup>d</sup>Rocket thrust turned model in opposite direction following recovery.



CHART 1.- SPIN AND RECOVERY CHARACTERISTICS OF THE MODEL WITH THE SPIN-RECOVERY ROCKETEES INSTALLED

[Loading 1 in table II and figure 7; direction of spin as indicated; recovery attempted by rapid full rudder reversal except as indicated (recovery attempted from, and steady-spin data presented for, rudder-full-with spins); erect spins]



aVisual estimate.

bRecovery attempted by rudder reversal from full with to  $\frac{2}{3}$  against the spin.

cModel entered an aileron roll.

dOscillatory spin, range of values given.

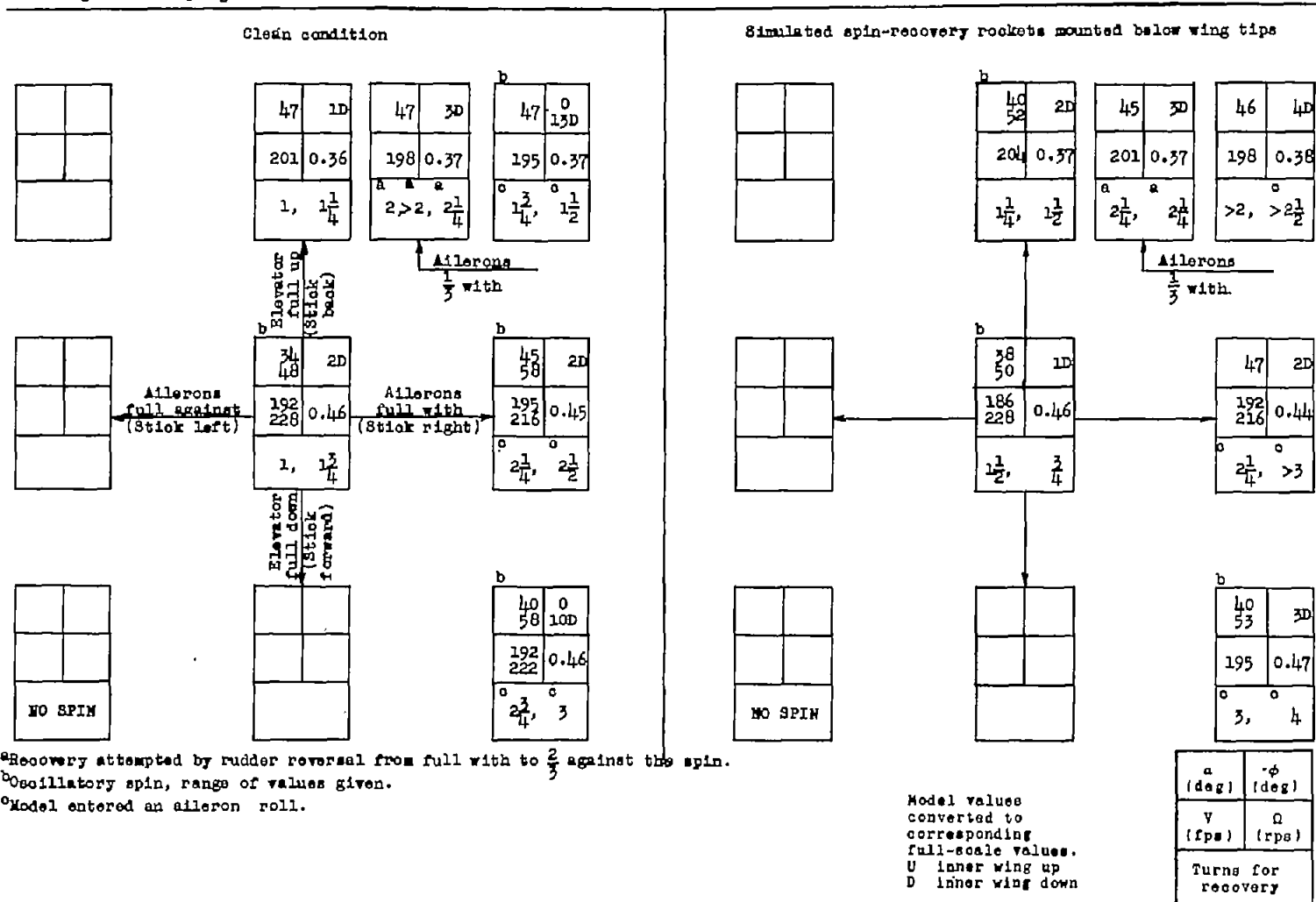
eRecovery attempted by simultaneous rudder reversal from full with to  $\frac{2}{3}$  against the spin and elevator movement from  $\frac{2}{3}$  up to  $\frac{1}{2}$  down.

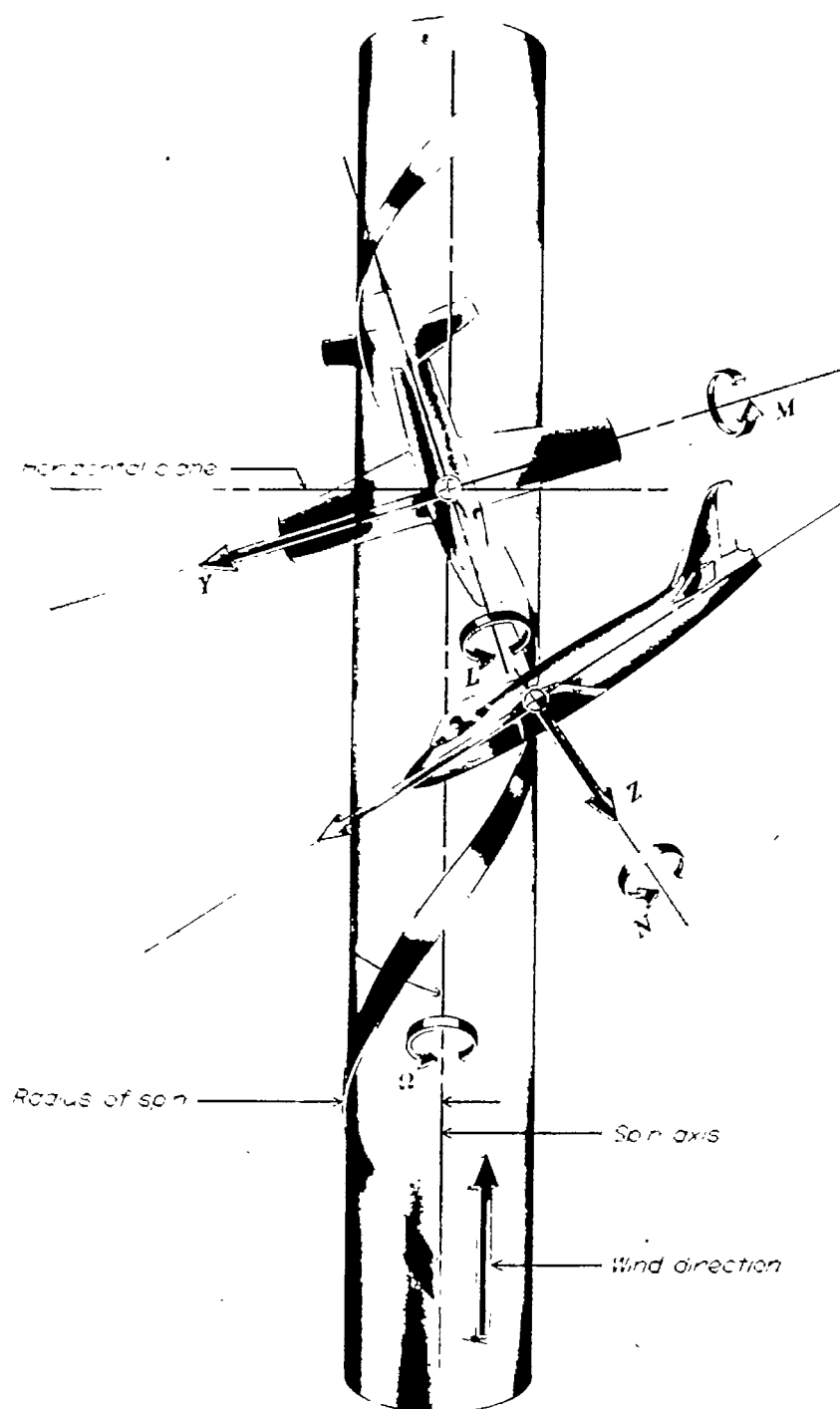
Model values converted to corresponding full-scale values.  
U inner wing up  
D inner wing down

$\alpha$ (deg)	$\phi$ (deg)
$V$ (fps)	$\Omega$ (rps)
Turns for recovery	

CHART 2.- SPIN AND RECOVERY CHARACTERISTICS OF THE MODEL IN THE CLEAN CONDITION AND WITH SIMULATED ROCKETS MOUNTED BELOW THE WING TIPS

[Loading 1 in table II and figure 7 (wing tips ballasted to retain mass distribution); recovery attempted by rapid full rudder reversal except as indicated (recovery attempted from, and steady-spin data presented for, rudder-full-with spins); right erect spin]





L-65735.1

Figure 1.- Illustration of an airplane in a spin. Arrows indicate positive directions of forces and moments along and about the body axes of the airplane.

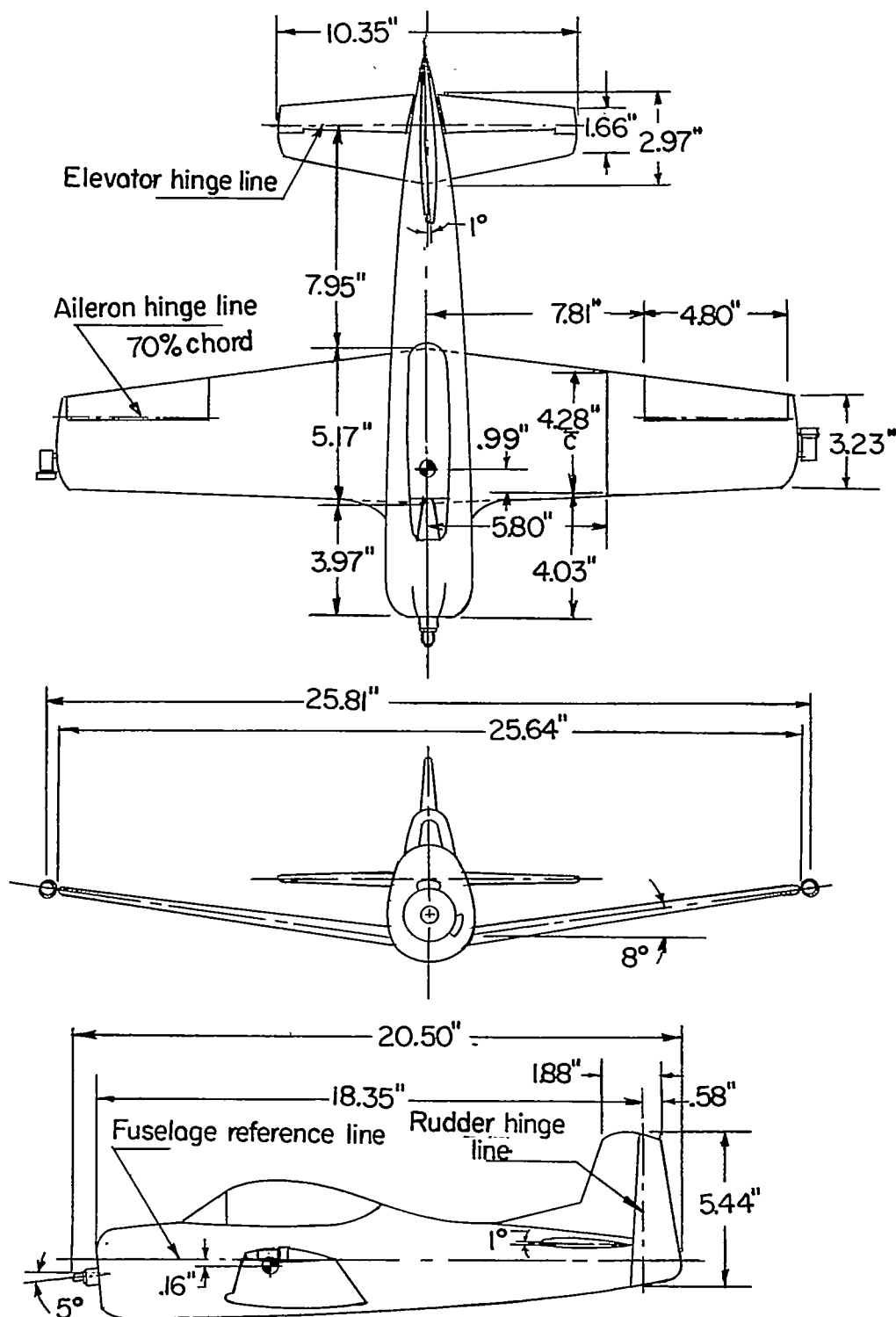


Figure 2.- Three-view drawing of the airplane represented by the 1/19-scale spin model. Wing incidence varied from  $2^\circ$  at root to  $-1^\circ$  at tip.

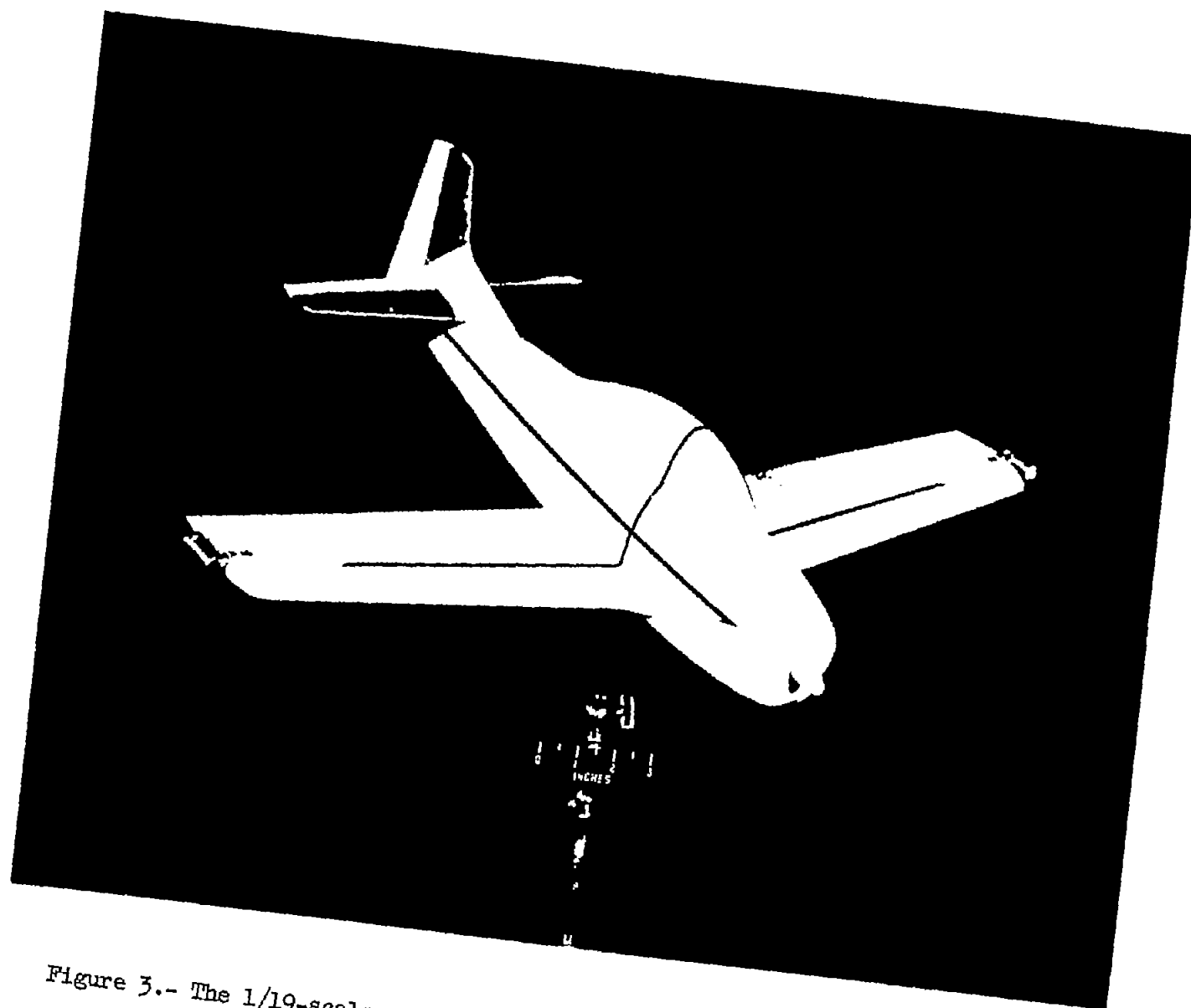
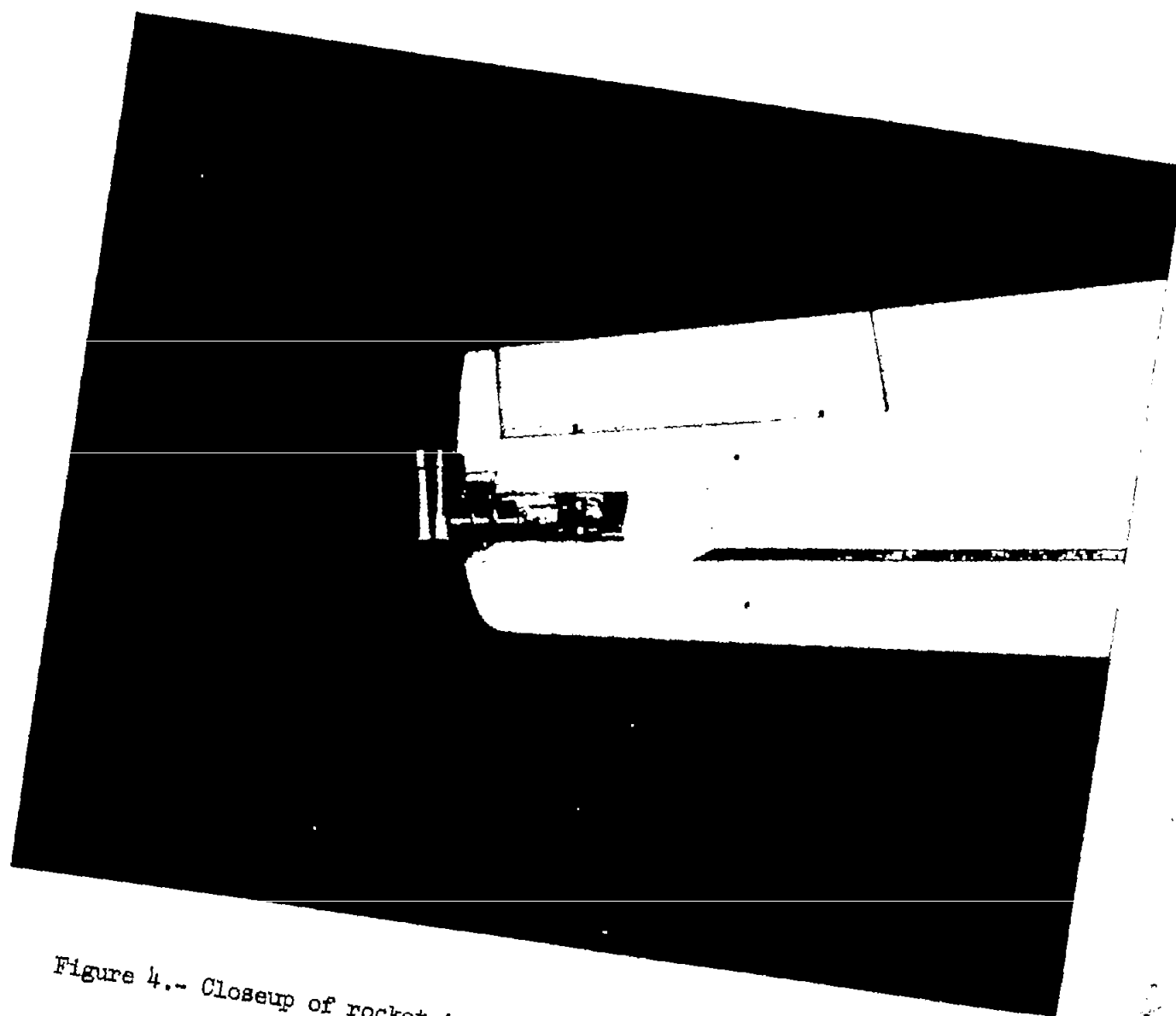


Figure 3.- The 1/19-scale model of a trainer airplane with rockets installed on wing tips.

L-78089

NACA TM 3068



L-78093  
Figure 4.-- Closeup of rocket installed on wing tip of 1/19-scale model  
of a trainer airplane.

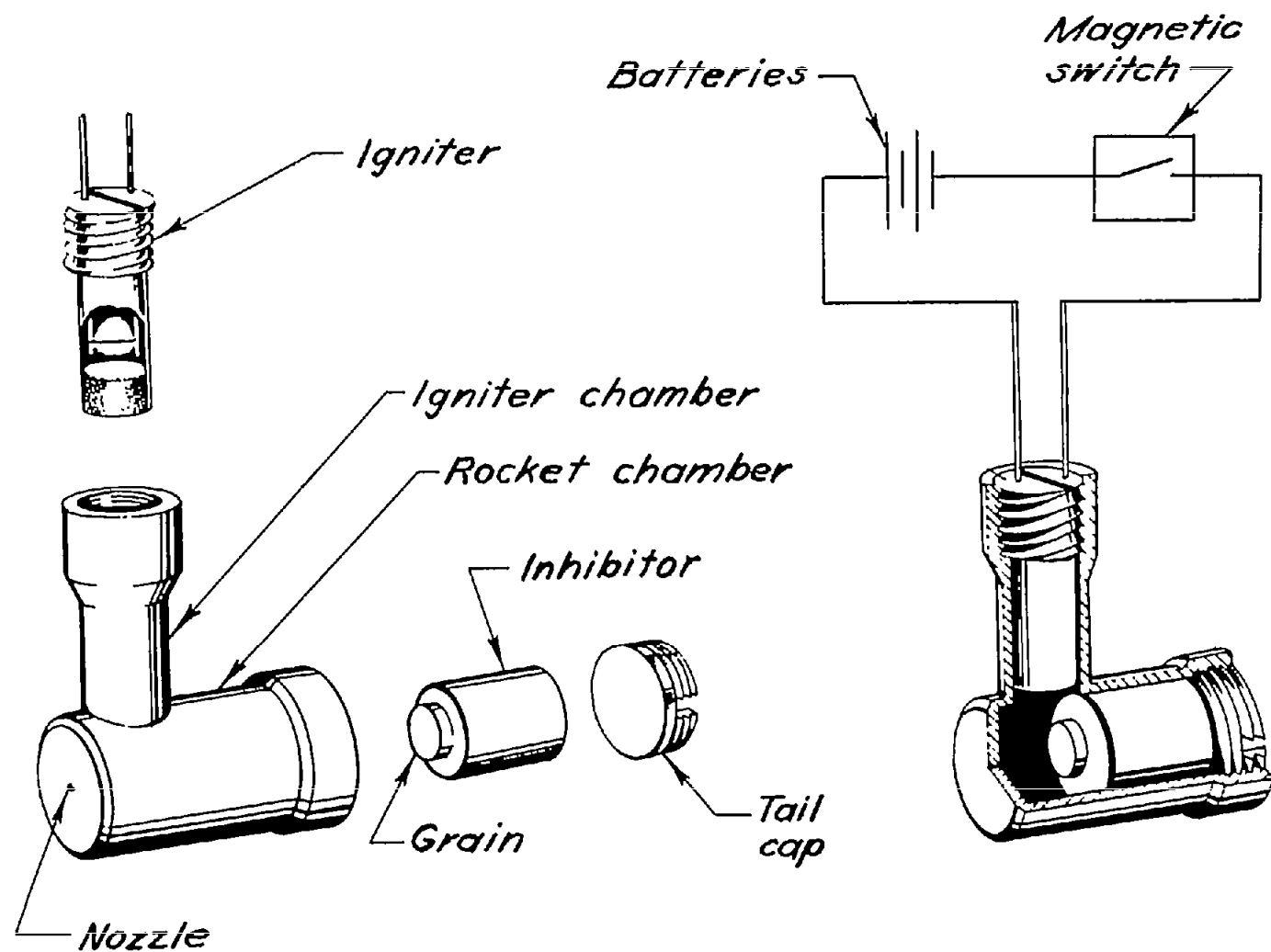


Figure 5.- Sketch of model rocket showing the various parts including the electrical circuit.

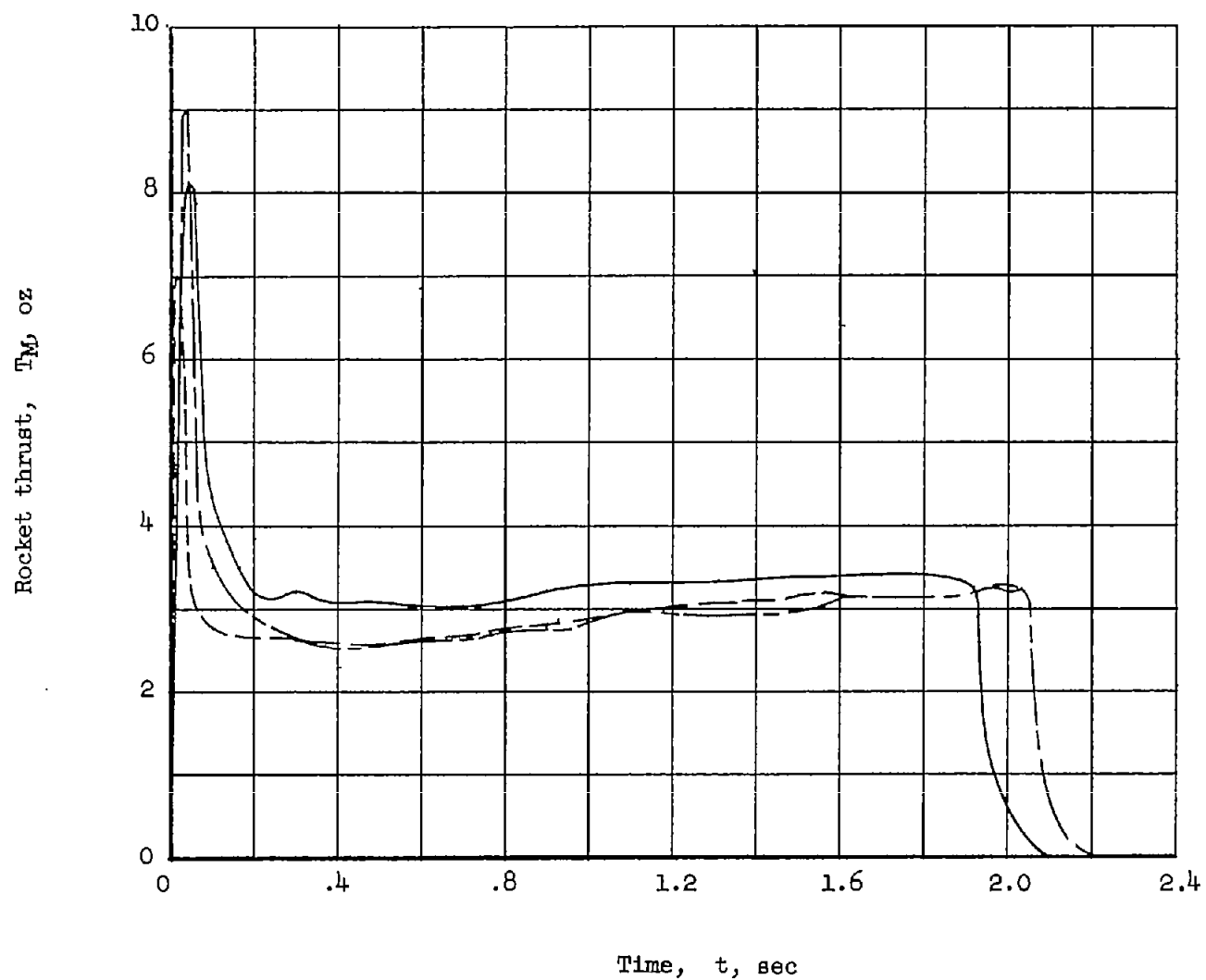


Figure 6.- Variation of model-rocket thrust with time for several rocket tests showing repeatability of firings.



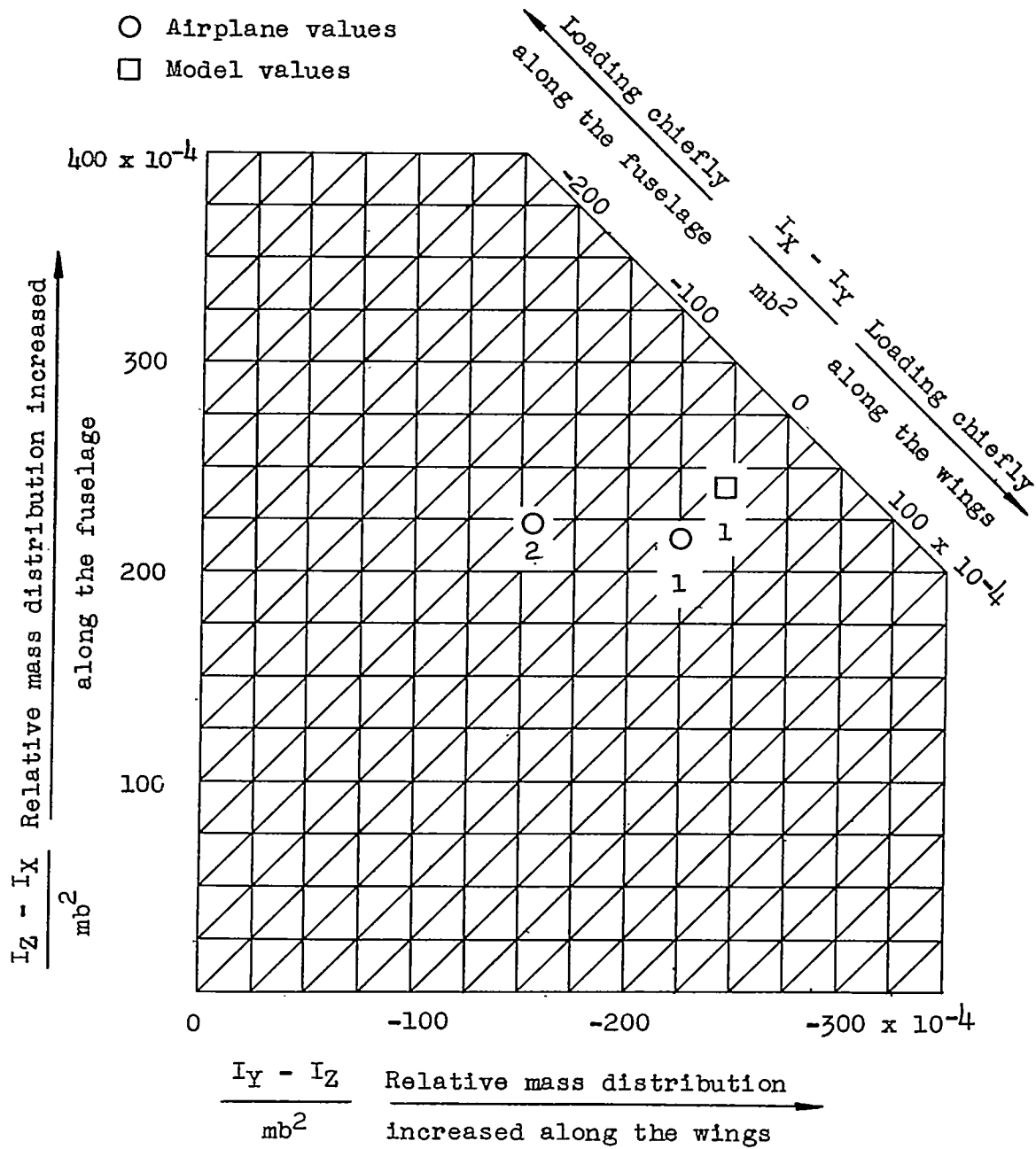


Figure 7.- Inertia parameters for loadings of the airplane and for the loading tested on the 1/19-scale model. (Numbers refer to loadings listed in table II.)

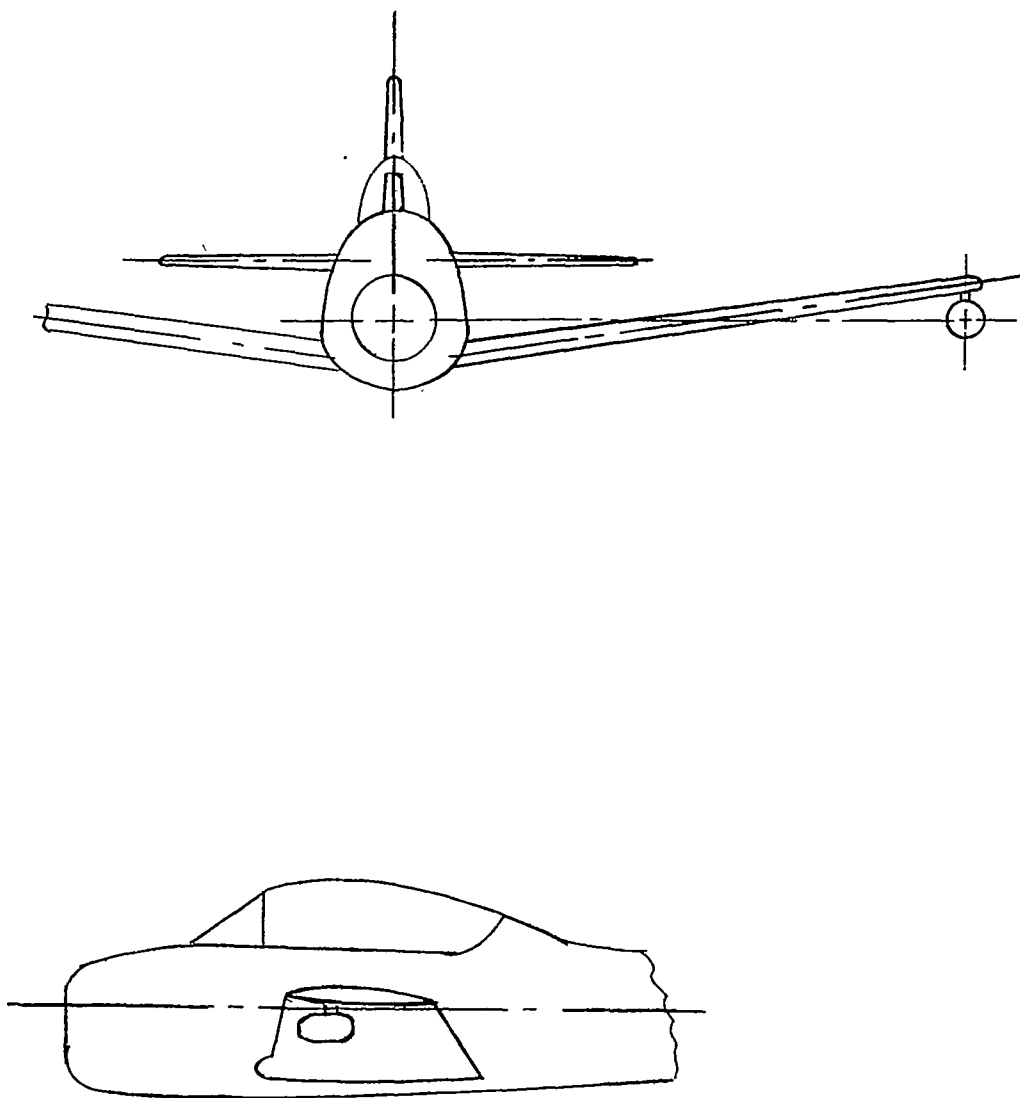


Figure 8.- Sketch of model showing dummy balsa rocket on lowered mount.

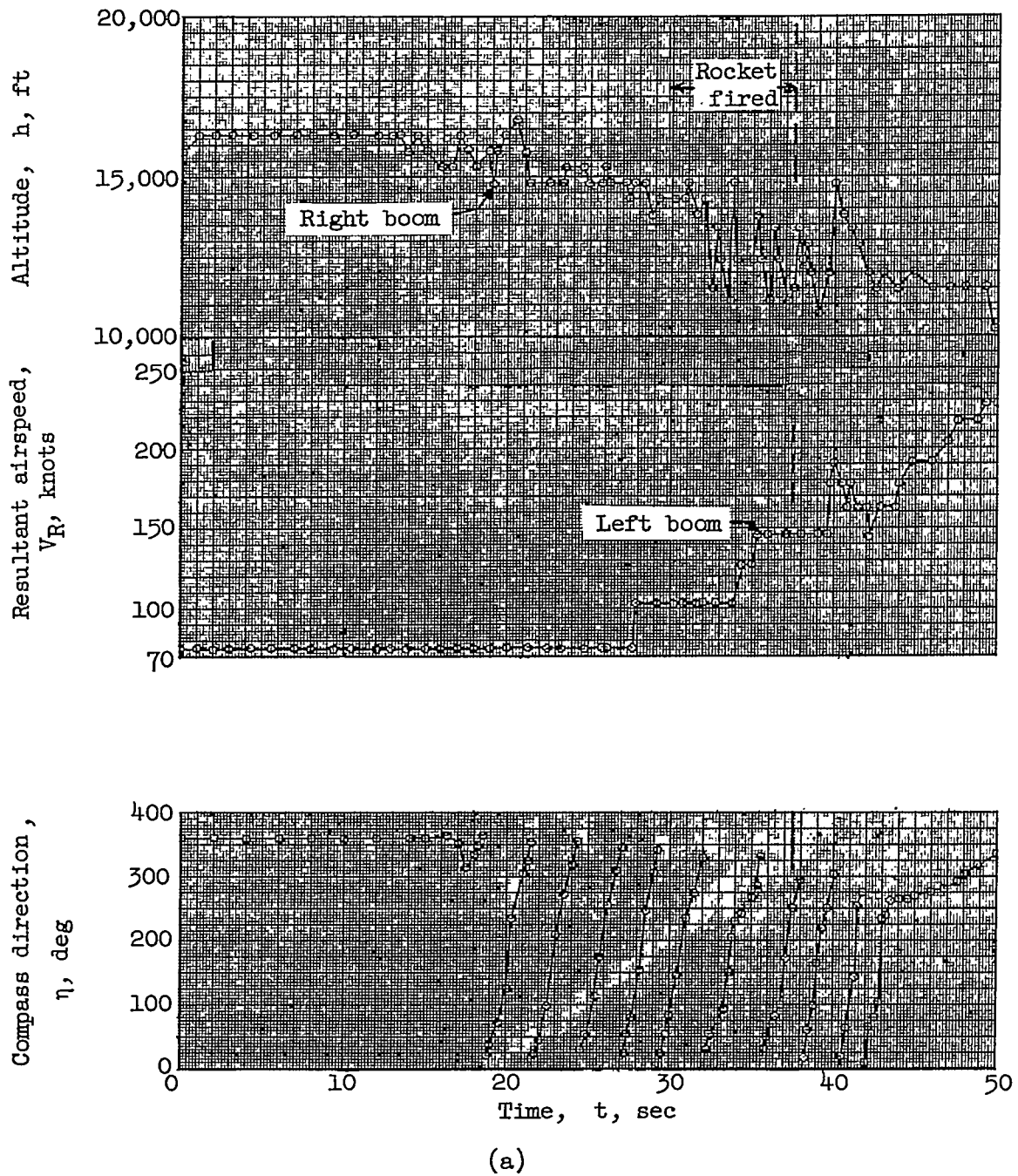
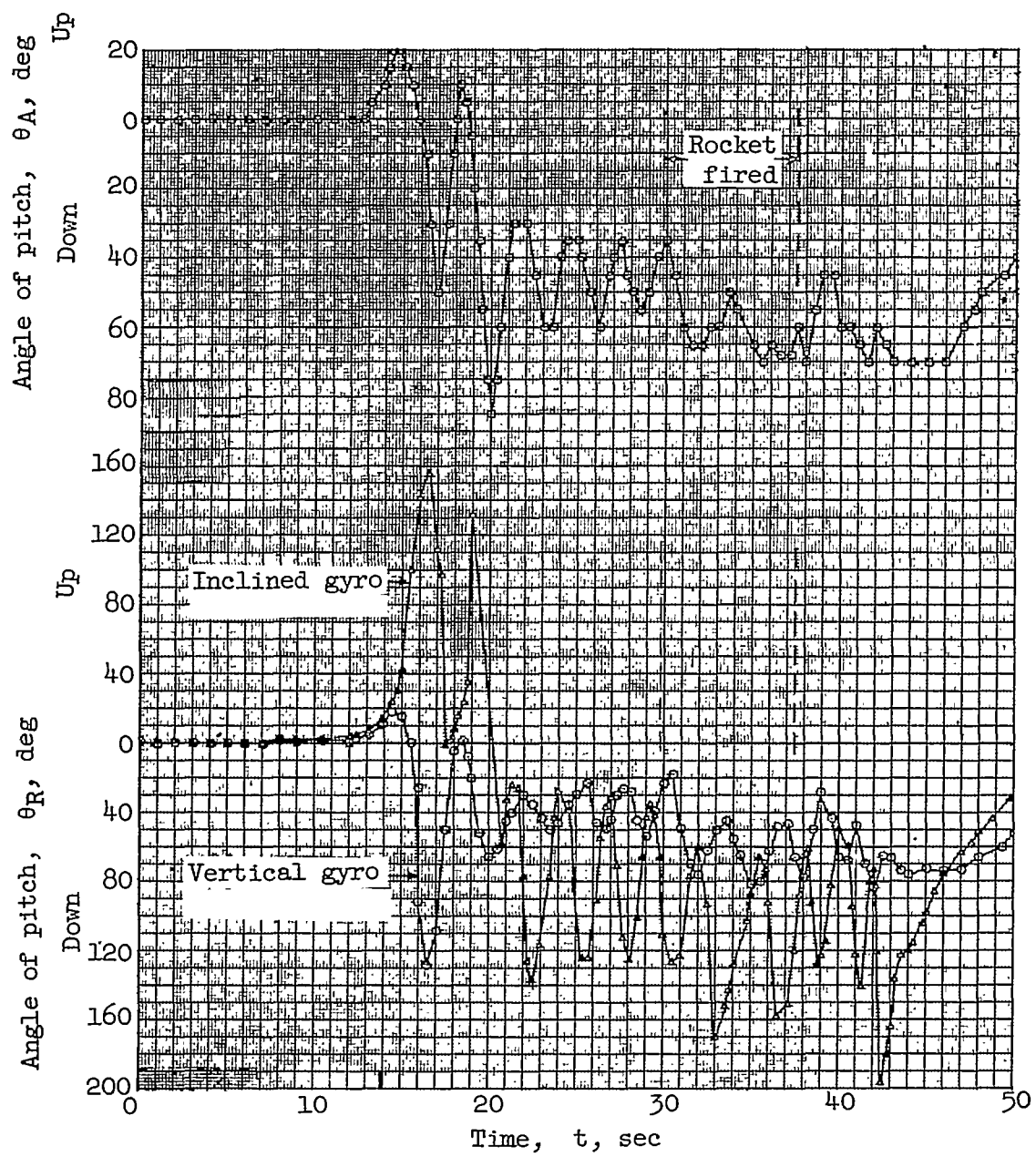
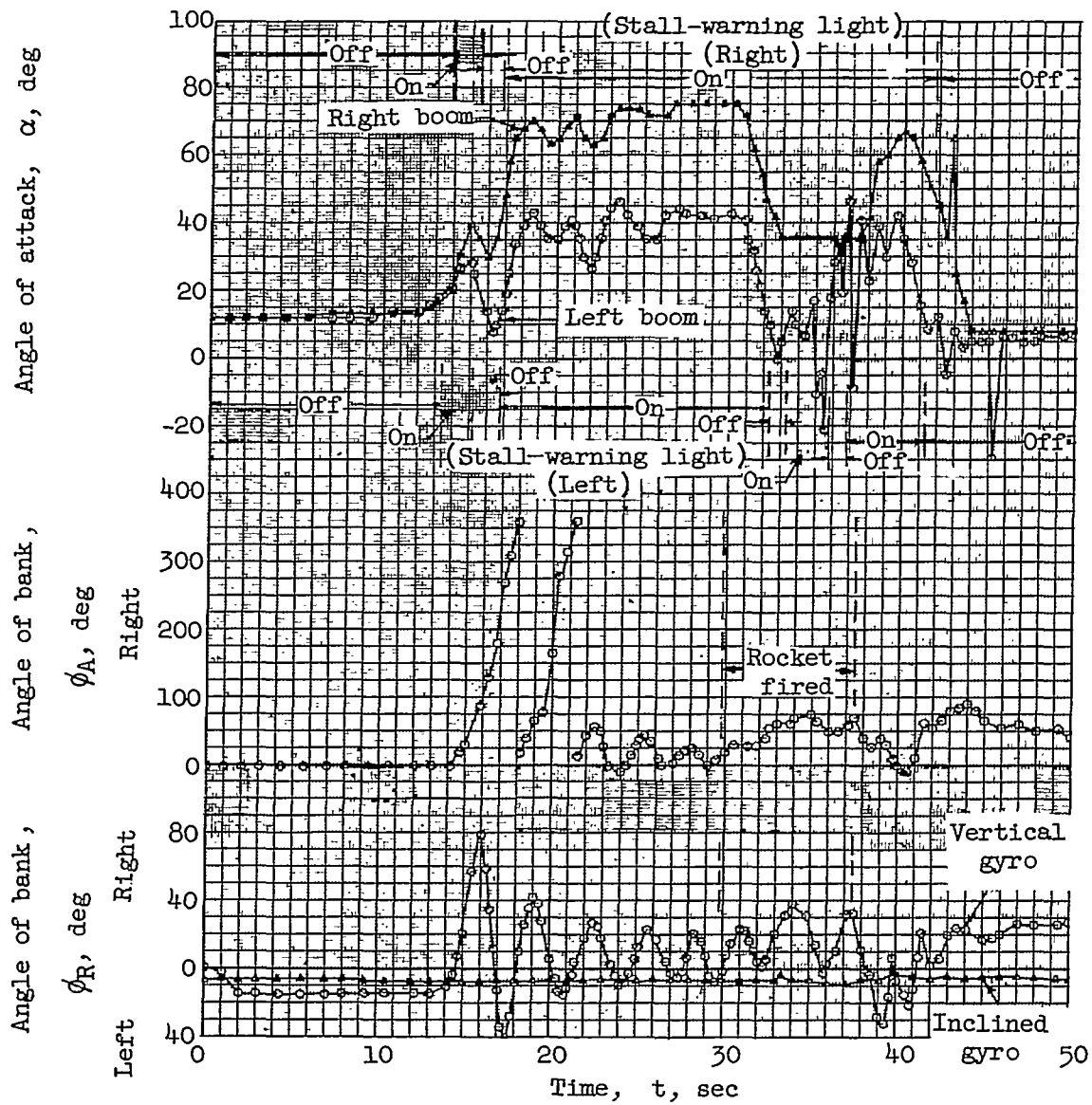


Figure 9.- Time history of airplane in a right spin. Recovery attempted by firing rocket mounted under right wing tip, thrust forward. Plots reproduced from reference 3.



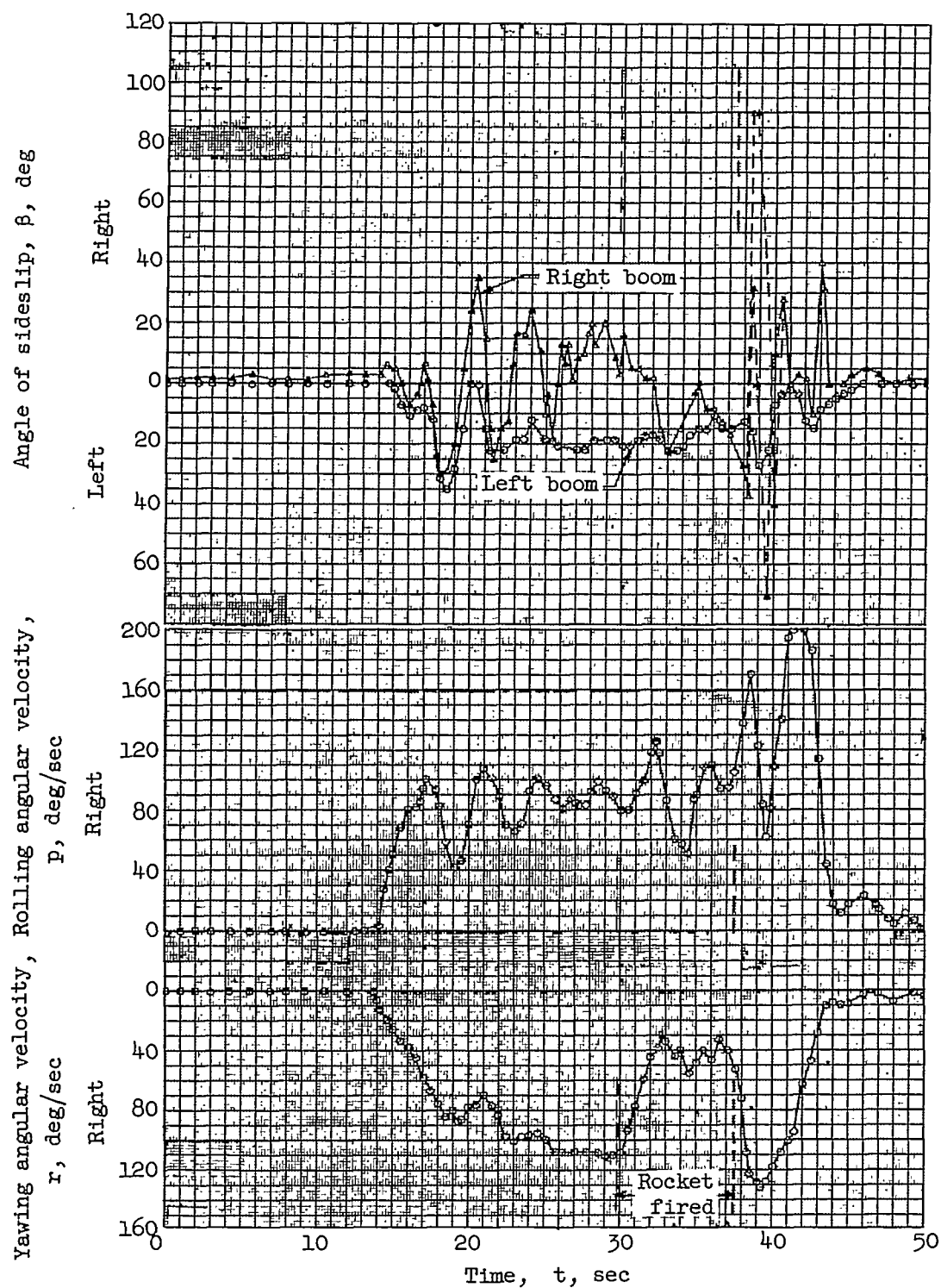
(b)

Figure 9.- Continued.



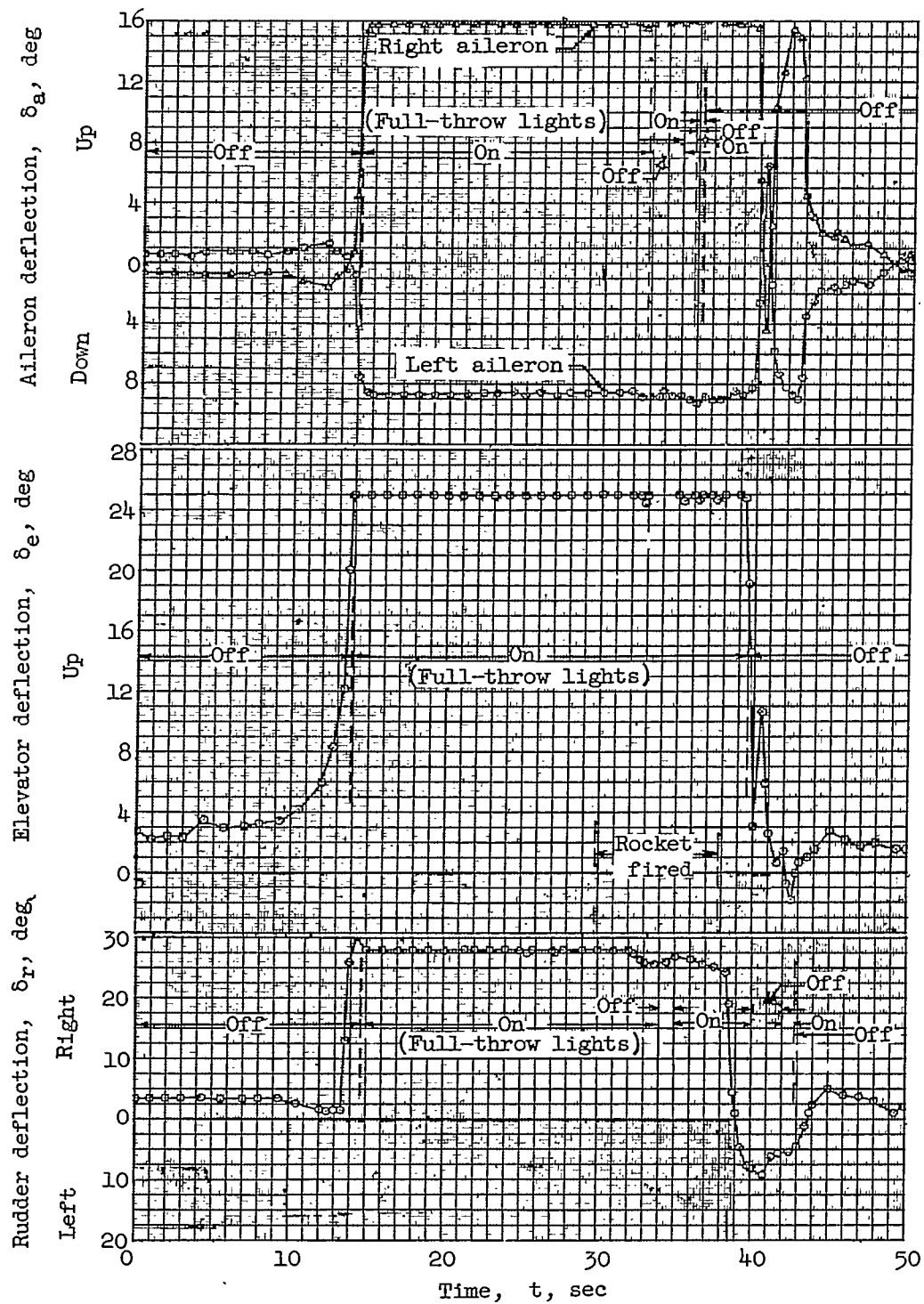
(c)

Figure 9.- Continued.



(d)

Figure 9.- Continued.



(e)

Figure 9.- Concluded.

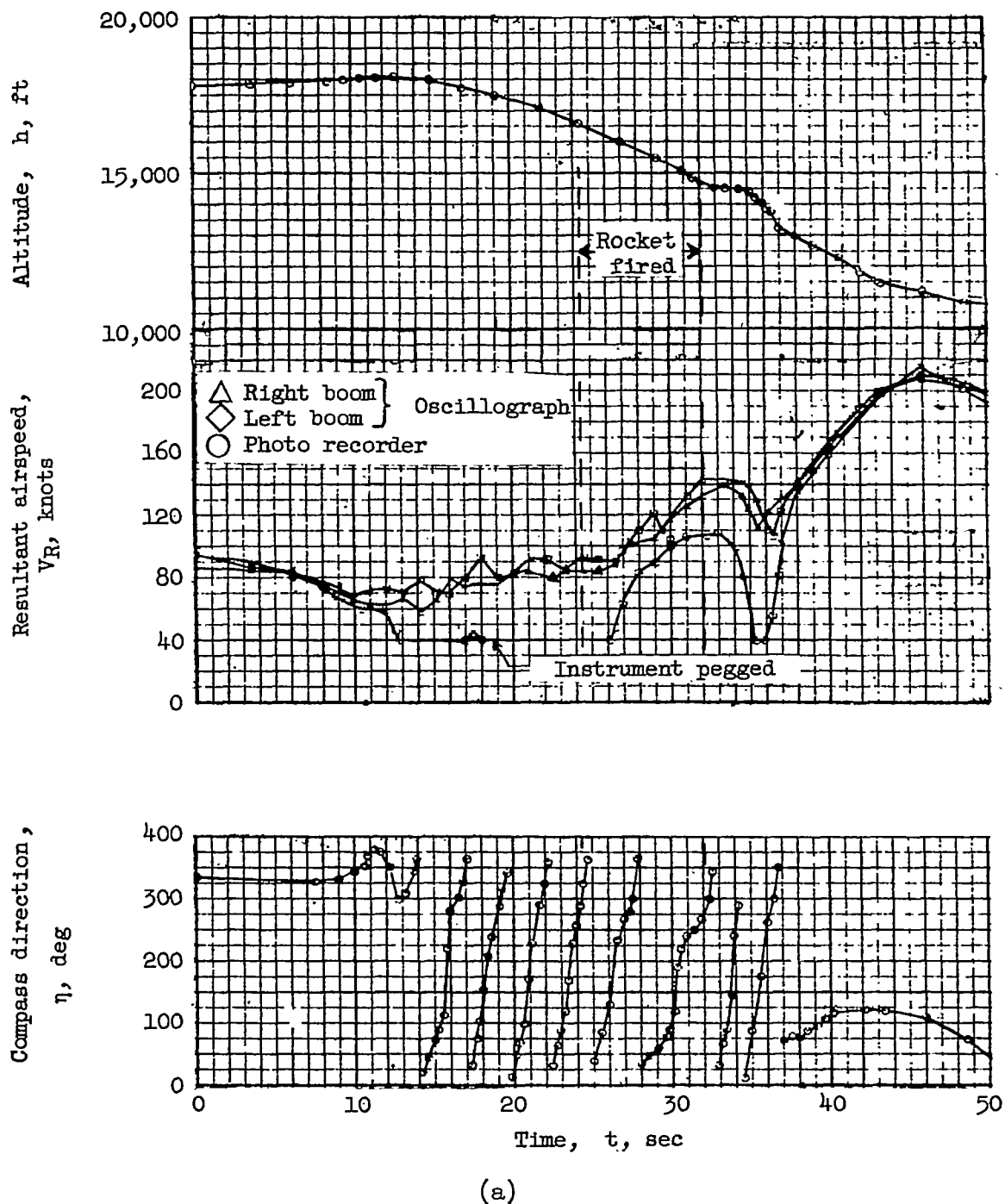
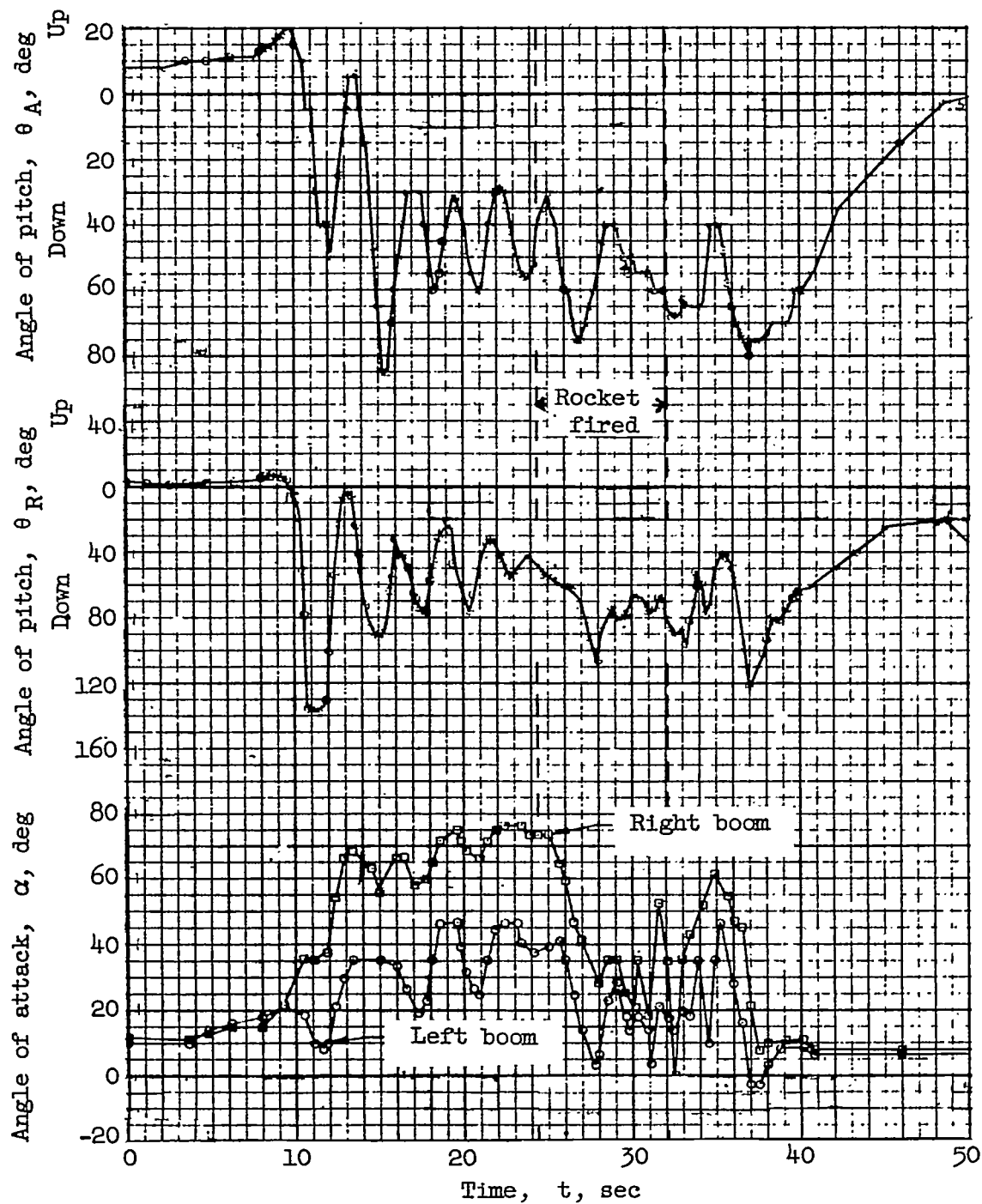


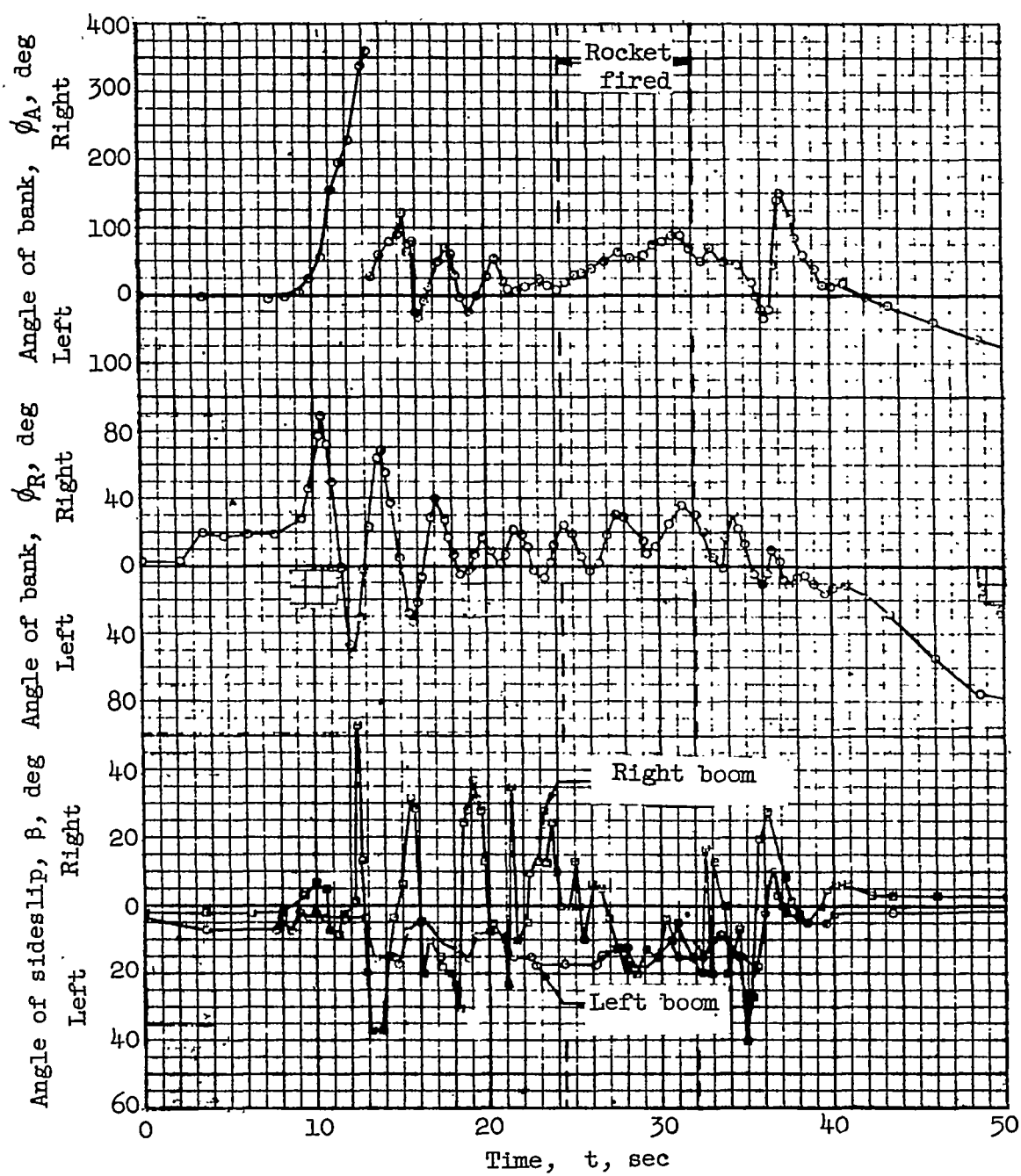
Figure 10.- Time history of airplane in a right spin. Recovery attempted by firing rocket mounted under right wing tip, thrust forward. Plots reproduced from reference 3.





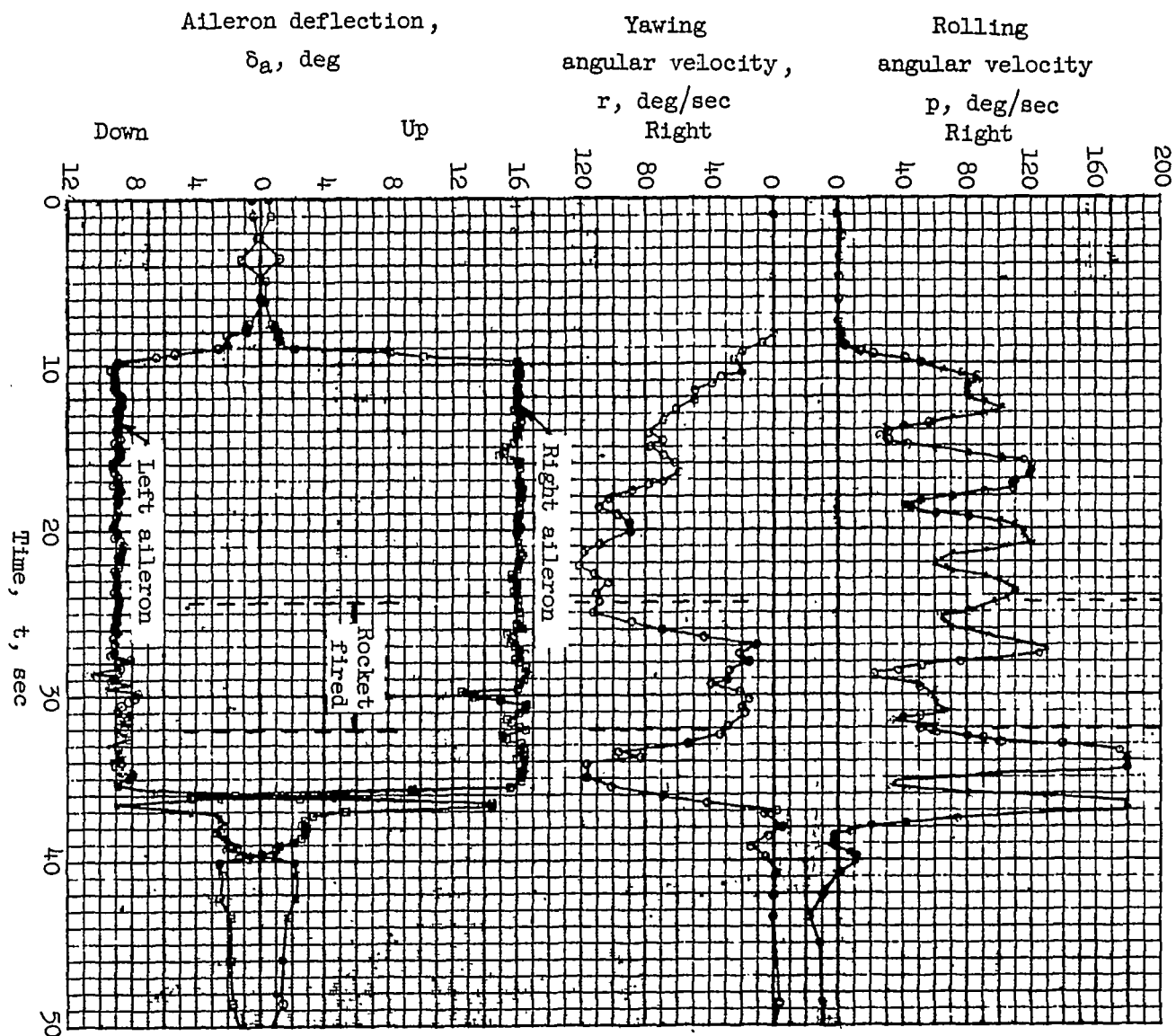
(b)

Figure 10.- Continued.



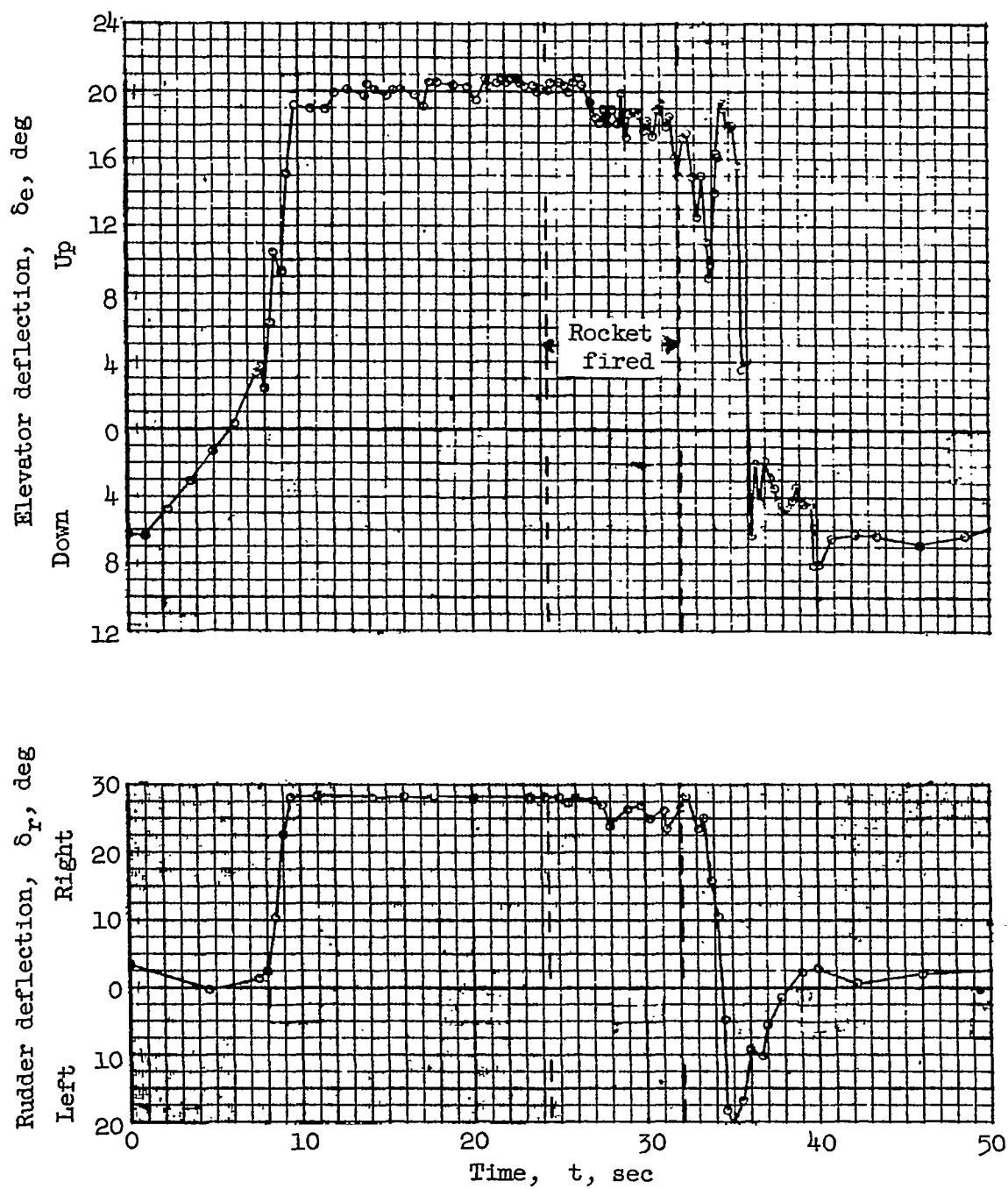
(c)

Figure 10.- Continued.



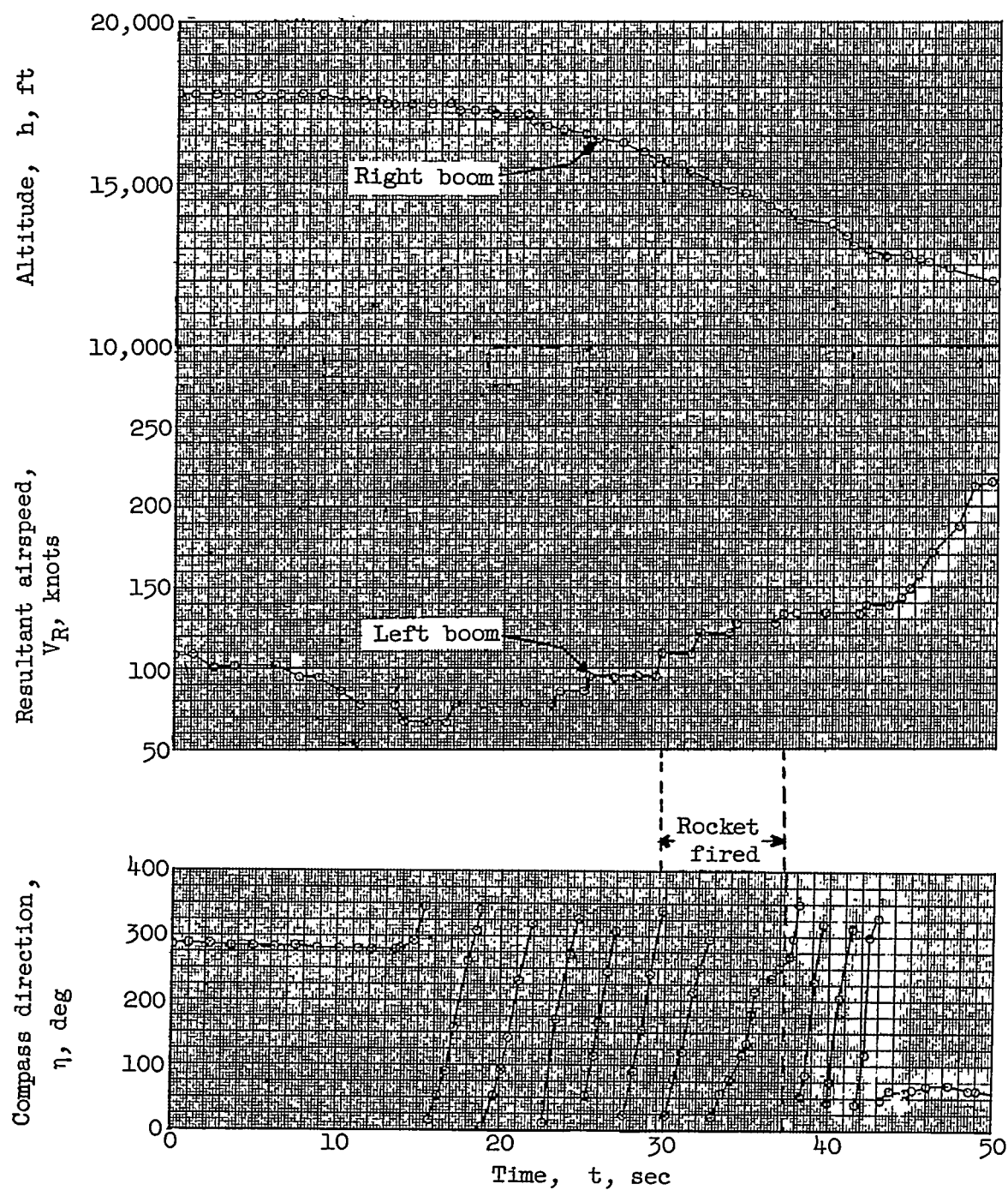
(a)

Figure 10.- Continued.



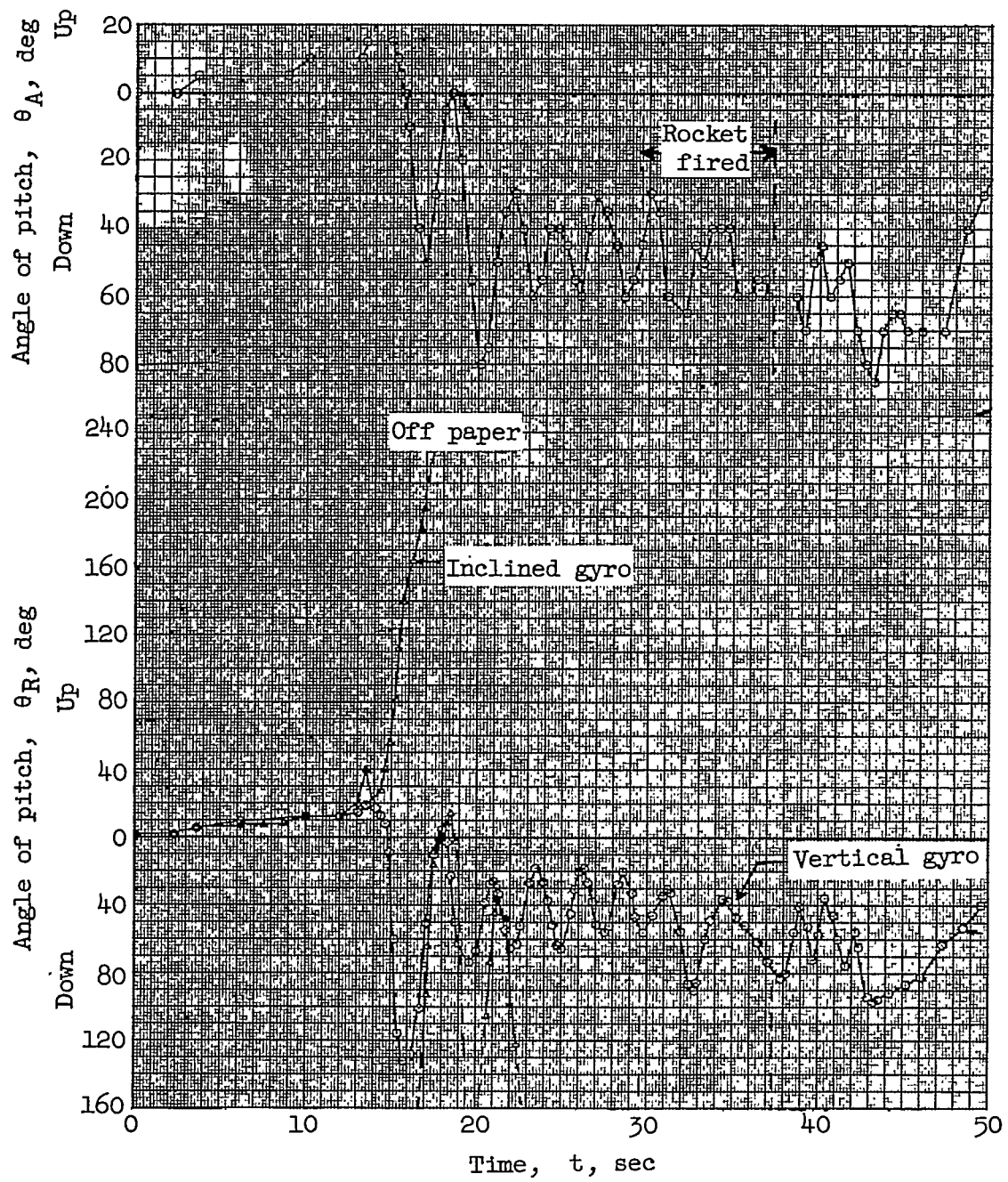
(e)

Figure 10.- Concluded.



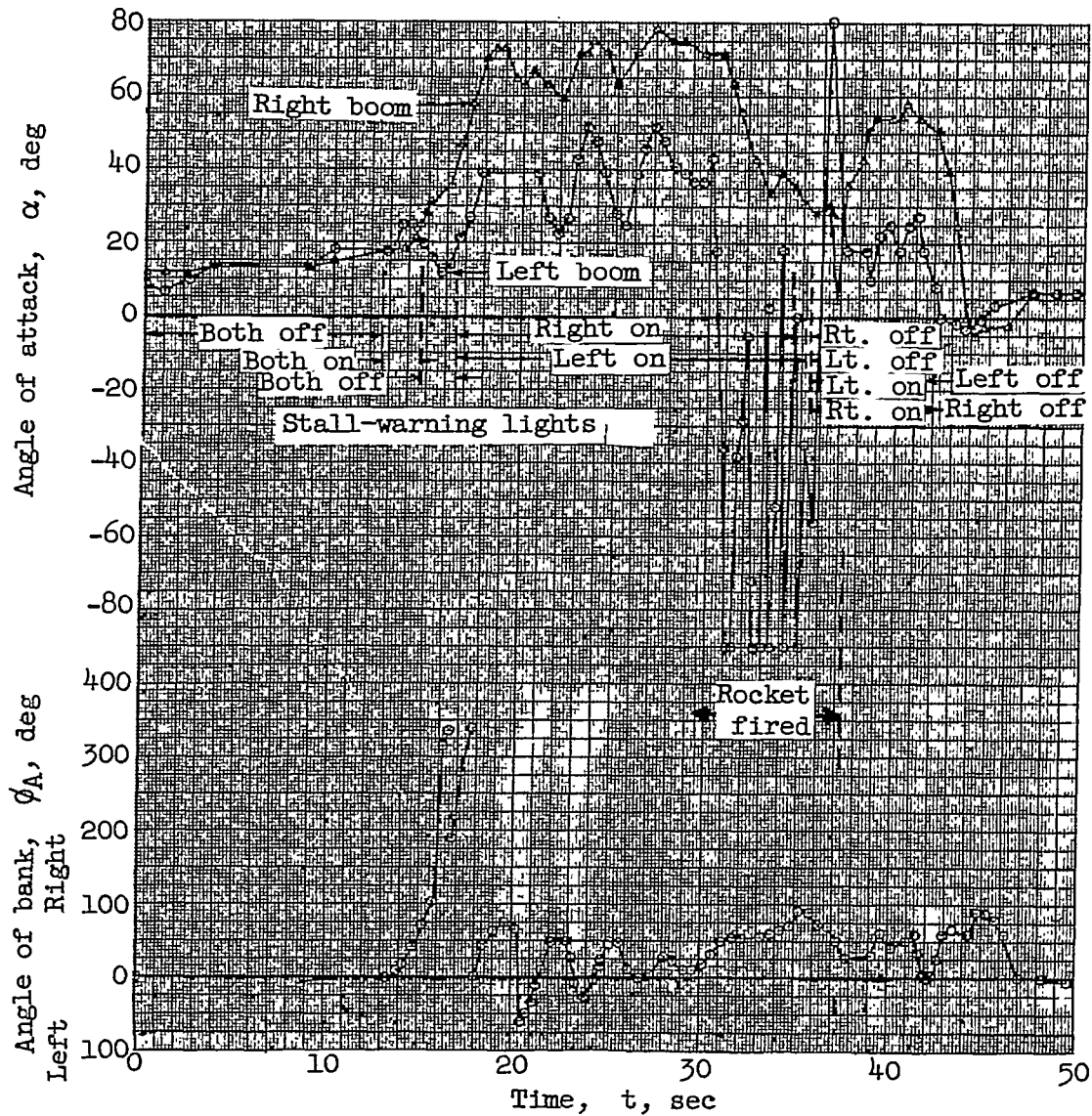
(a)

Figure 11.-- Time history of airplane in a right spin. Recovery attempted by firing rocket mounted under left wing tip, thrust rearward. Plots reproduced from reference 3.



(b)

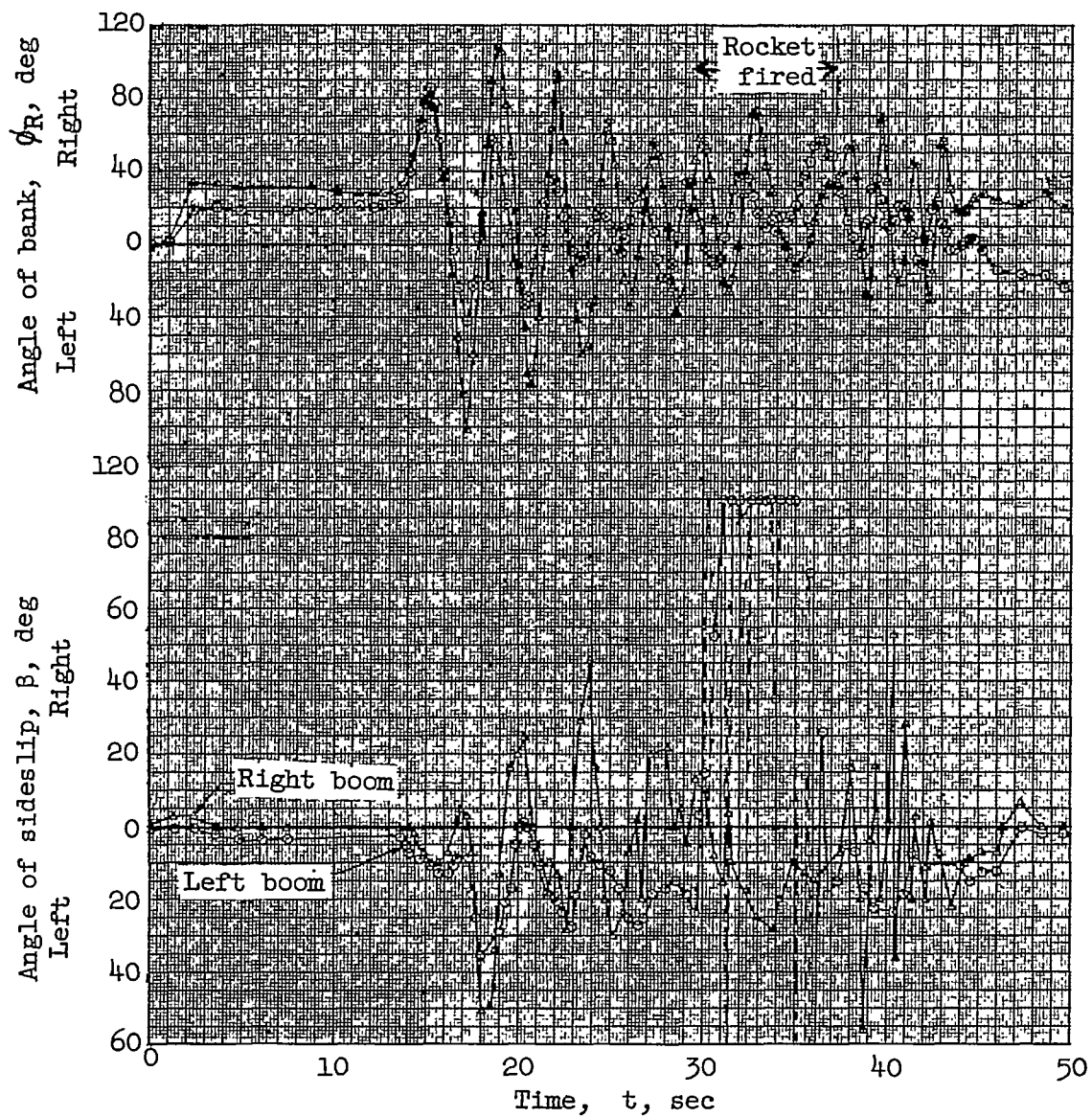
Figure 11.- Continued.



(c)

Figure 11.- Continued.

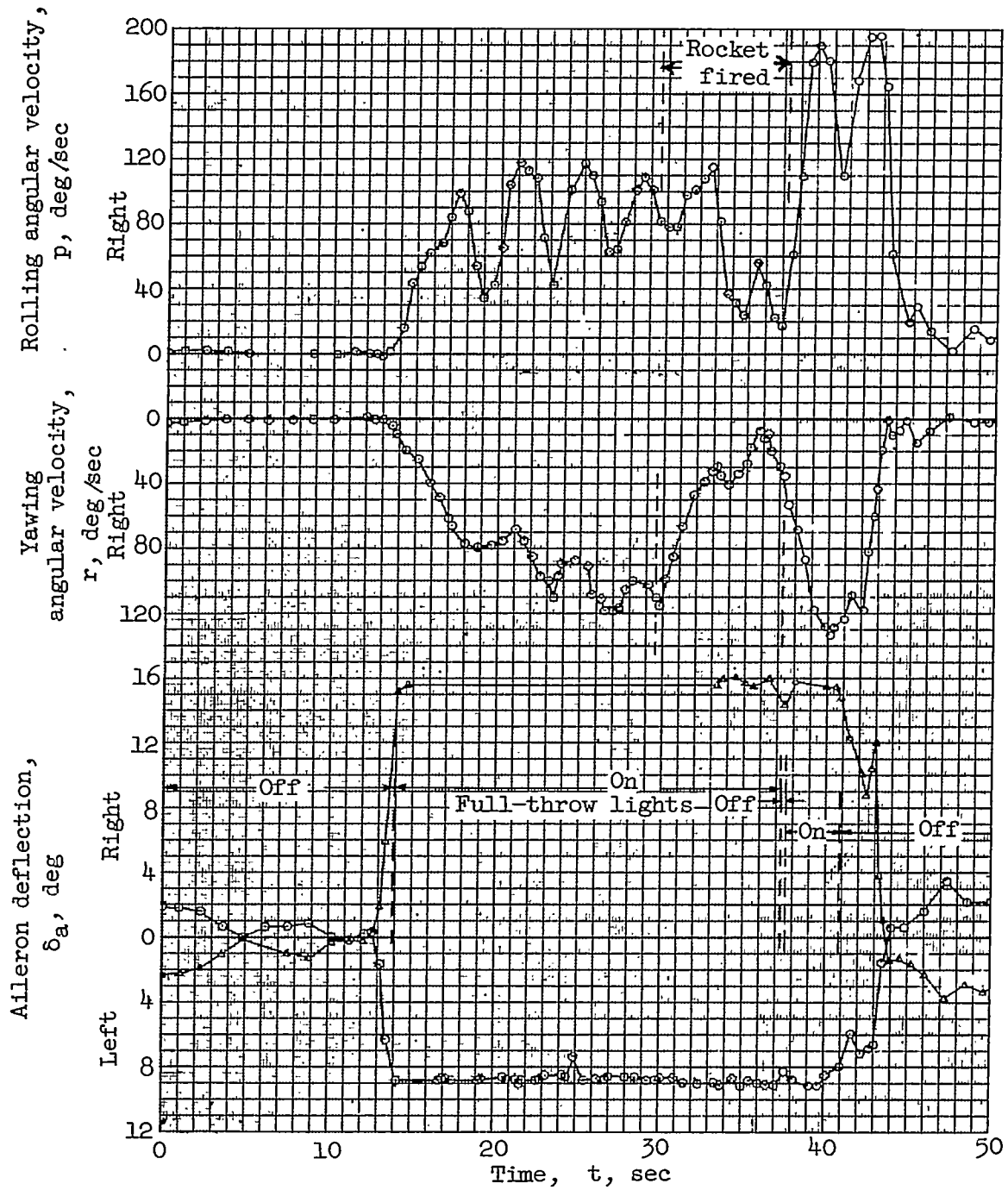




(d)

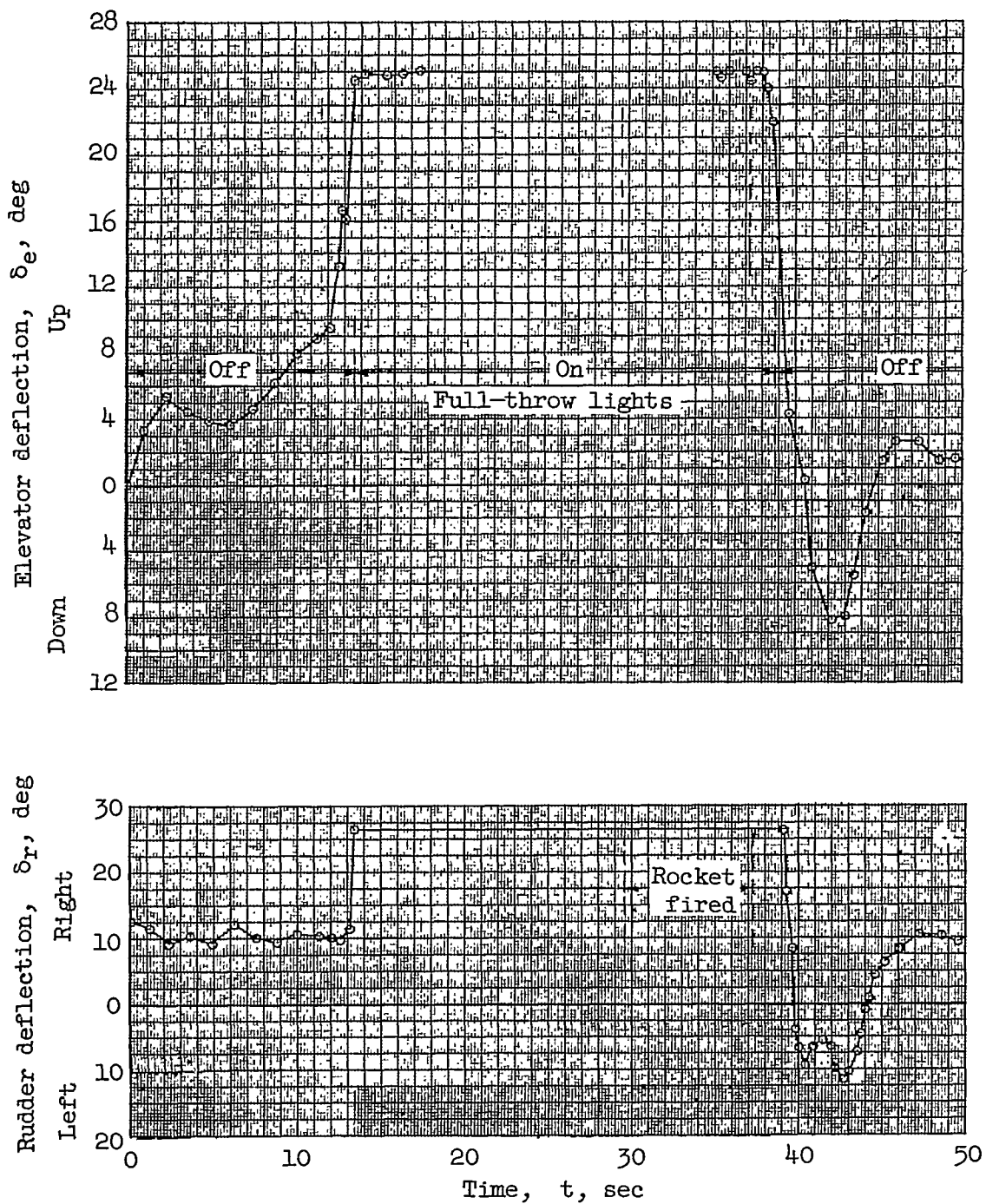
Figure 11.- Continued.





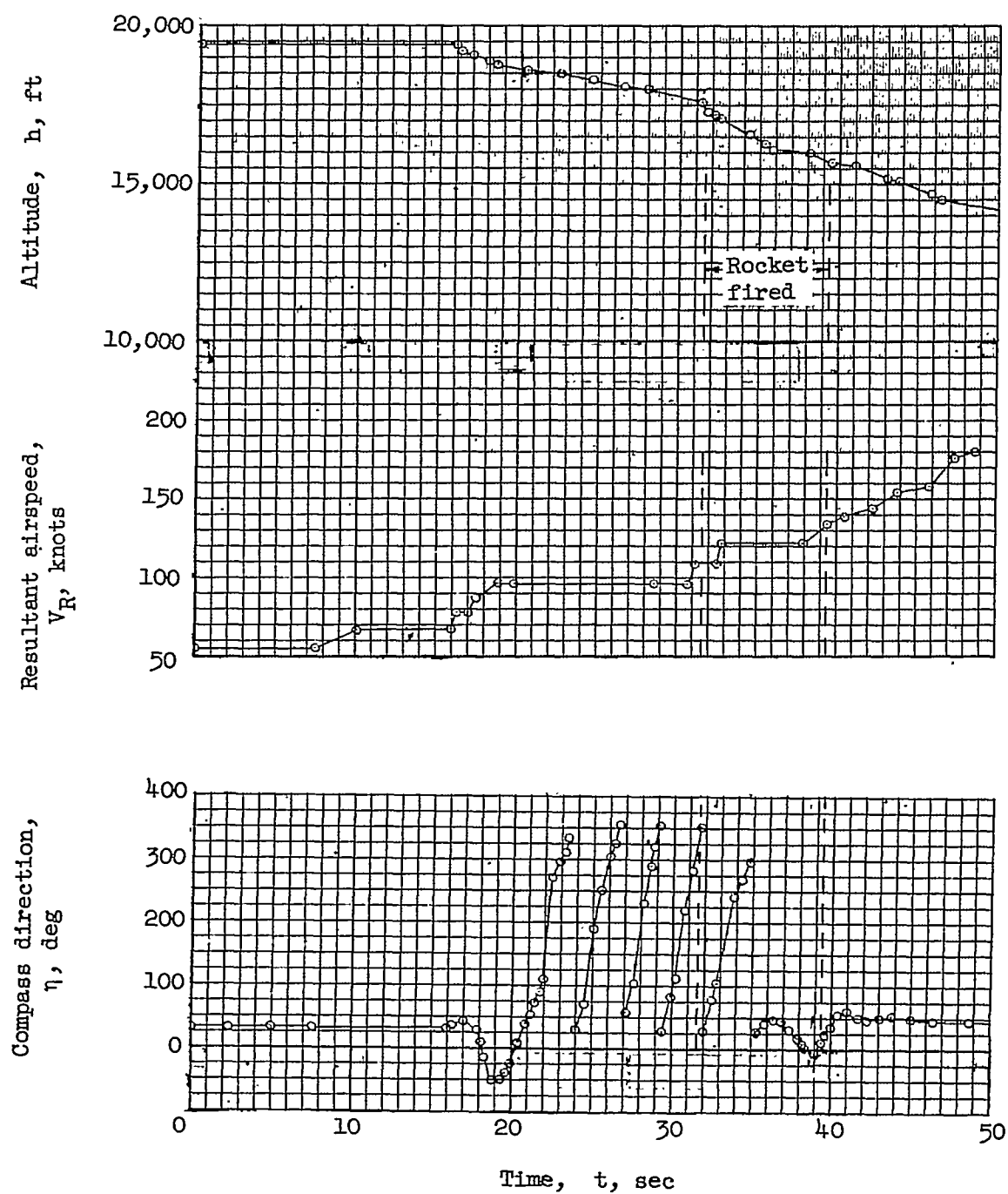
(e)

Figure 11.- Continued.



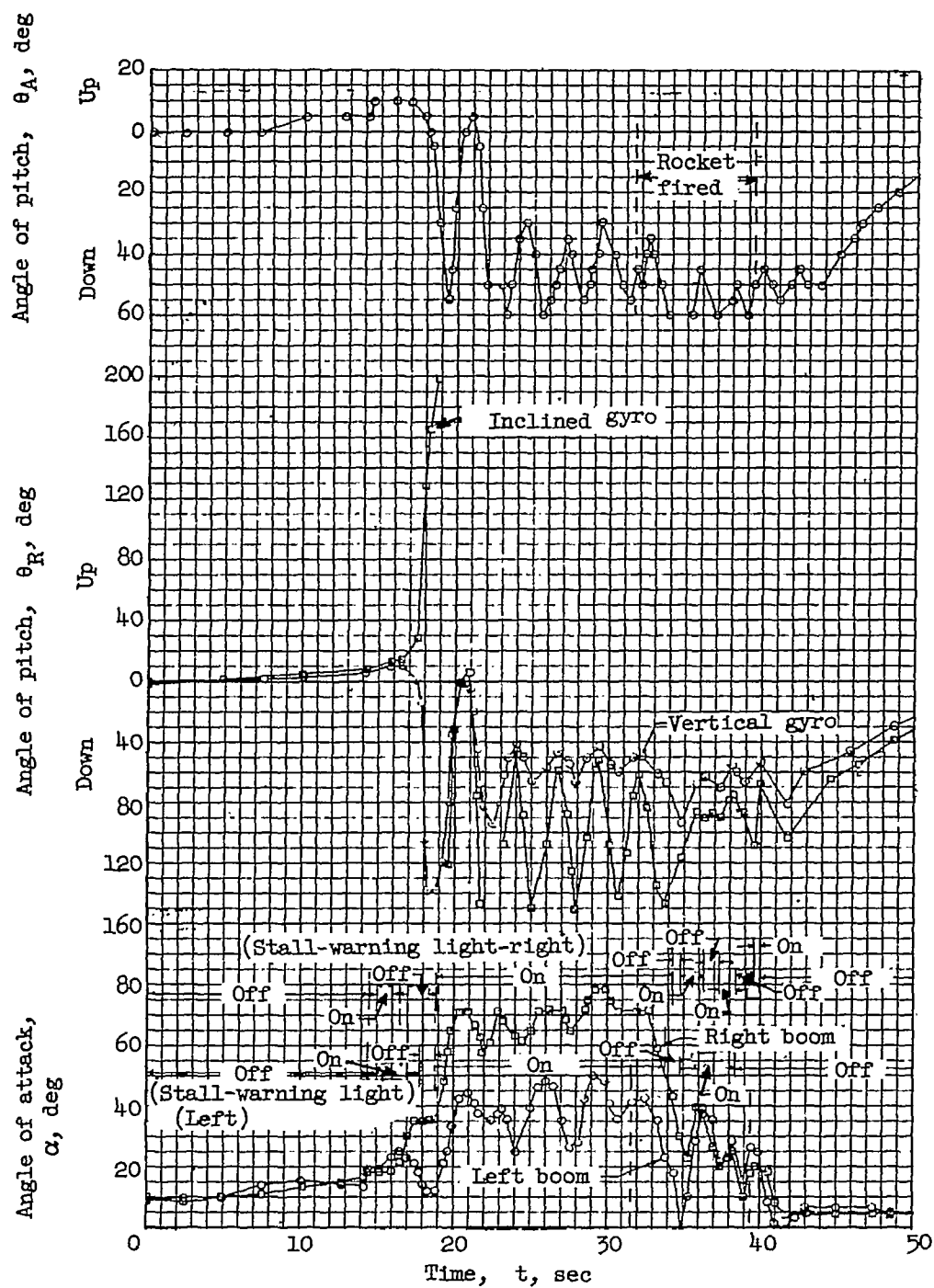
(f)

Figure 11.- Concluded.



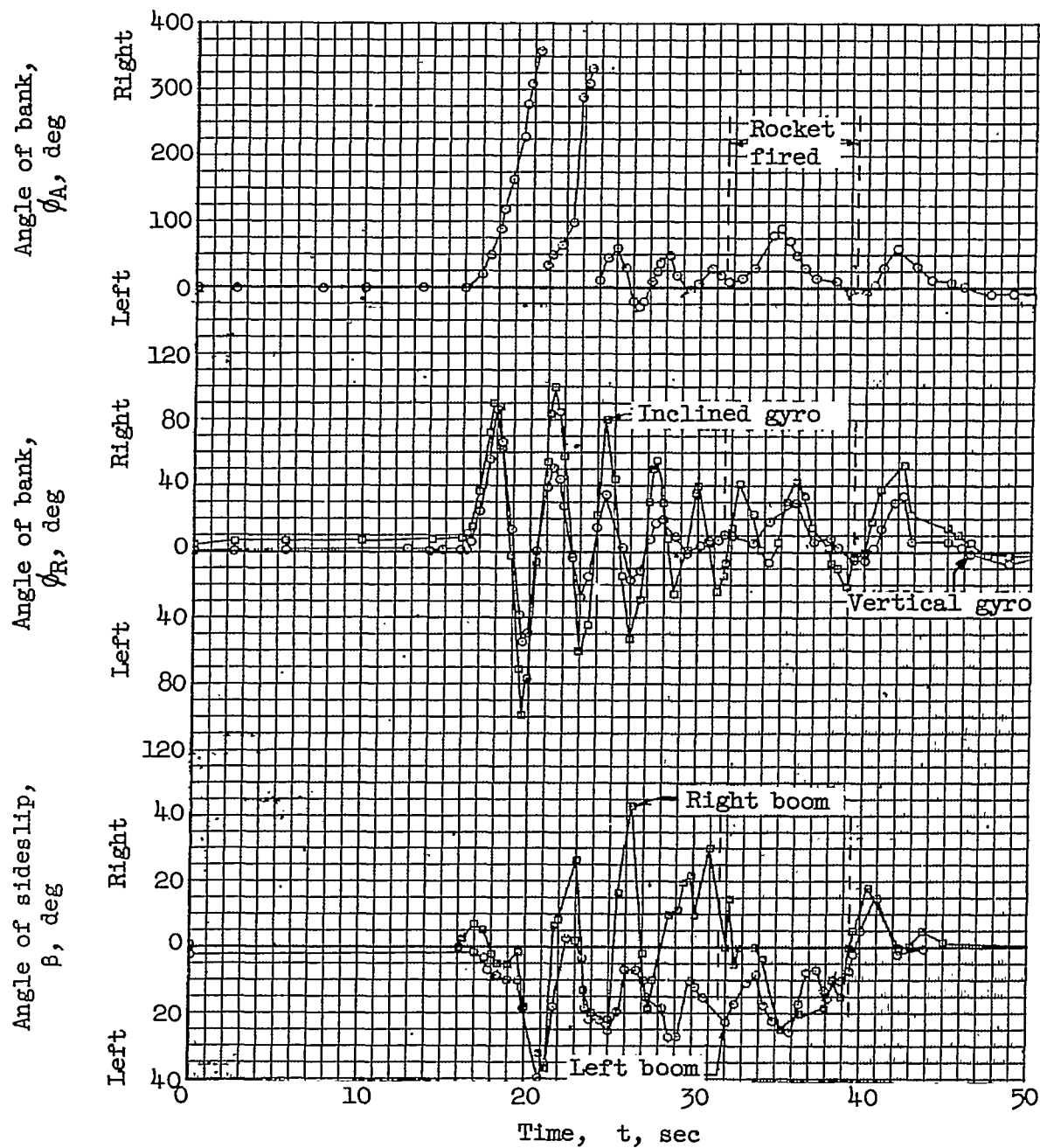
(a)

Figure 12.- Time history of airplane in a right spin. Recovery attempted by firing rocket mounted on left wing tip, thrust rearward. Plots reproduced from reference 3.



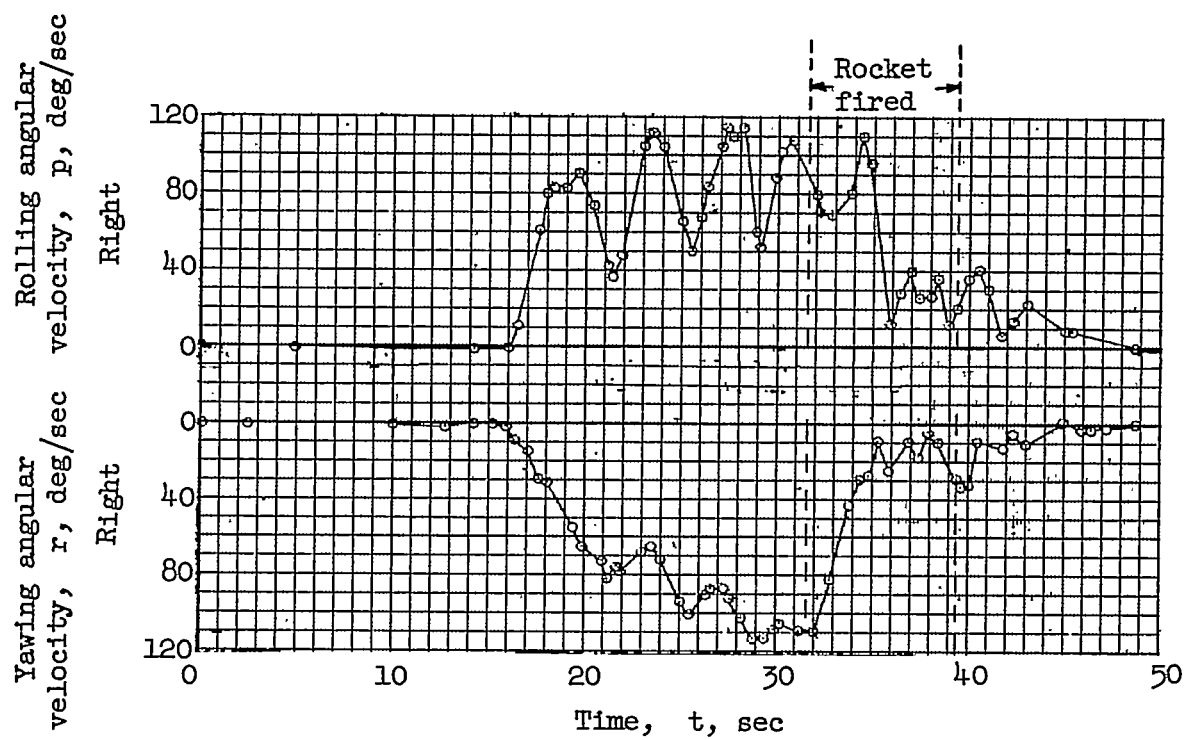
(b)

Figure 12.- Continued.



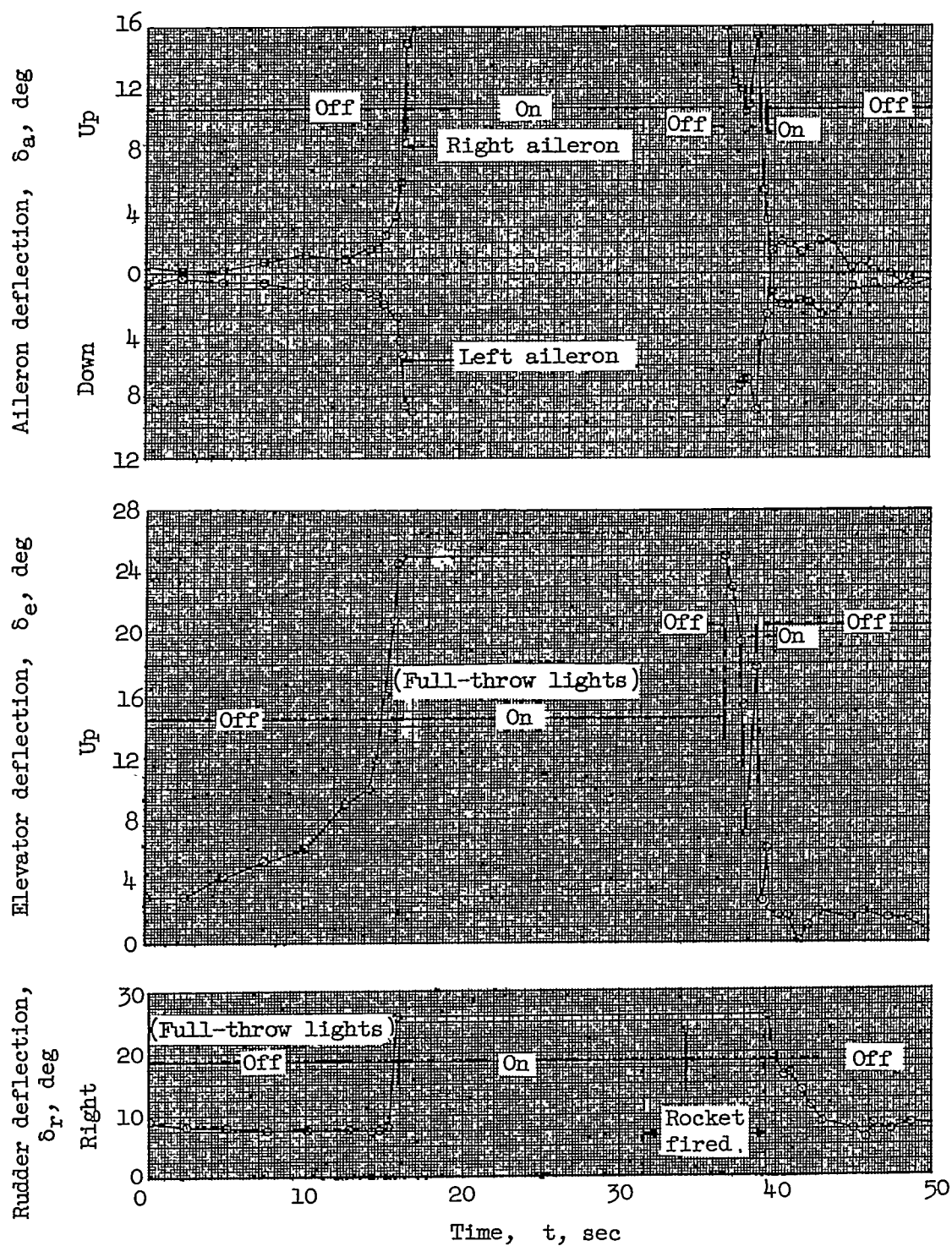
(c)

Figure 12.- Continued.



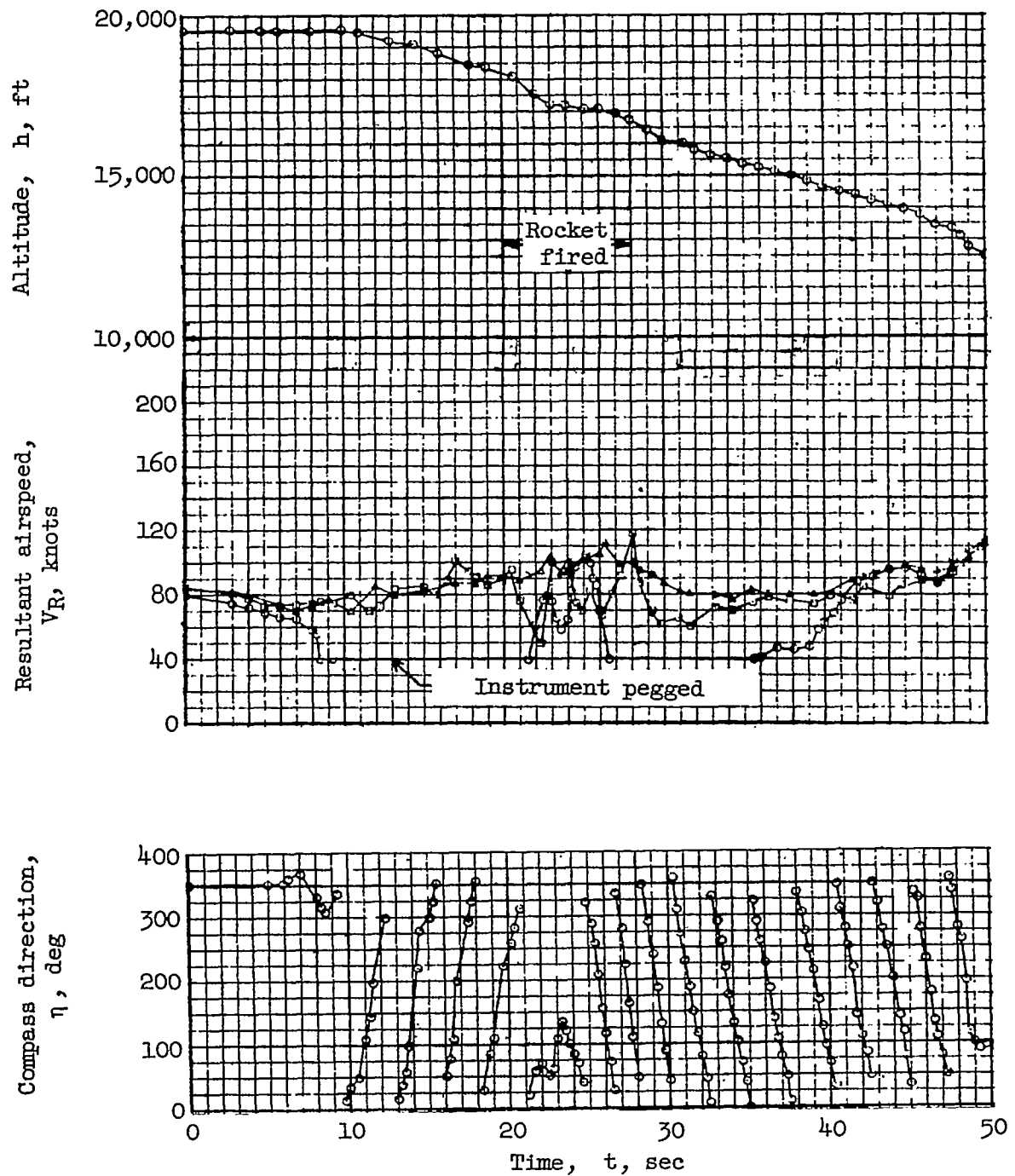
(d)

Figure 12.- Continued.



(e)

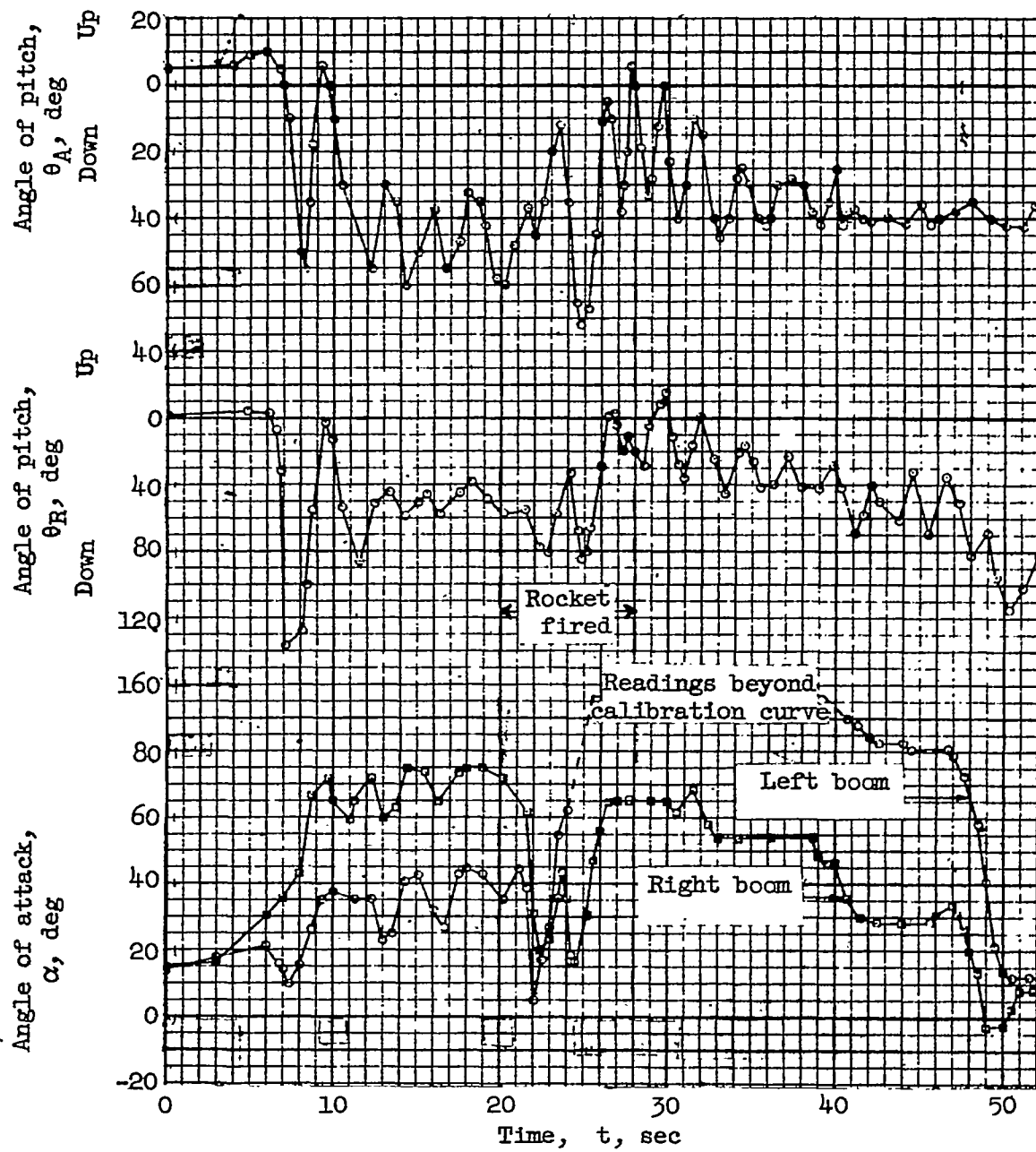
Figure 12.- Concluded.



(a)

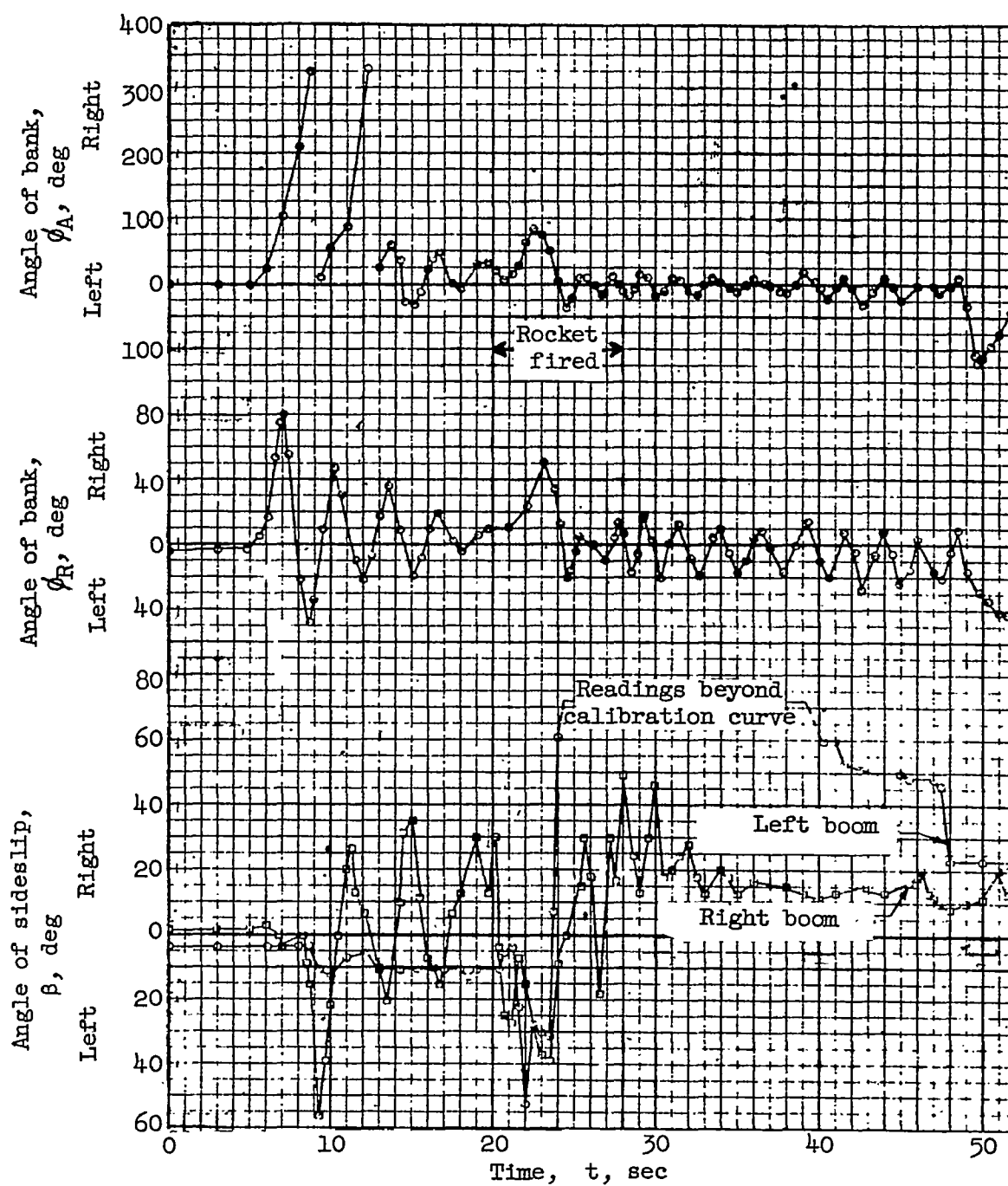
Figure 13.- Time history of airplane in a right spin. Recovery attempted by simultaneously firing both left and right rockets mounted below wing tip. Plots reproduced from reference 3.





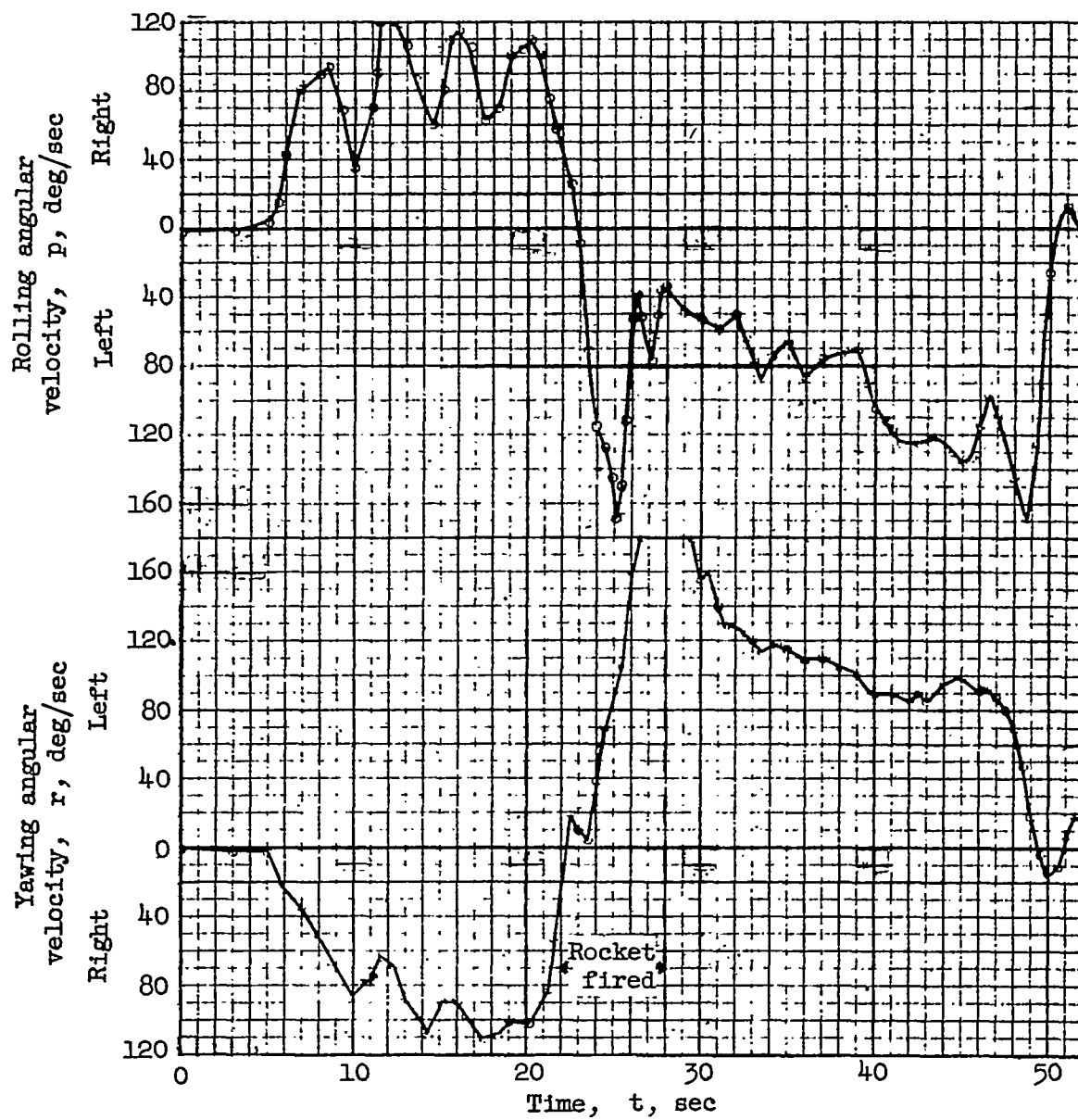
(b)

Figure 13.- Continued.



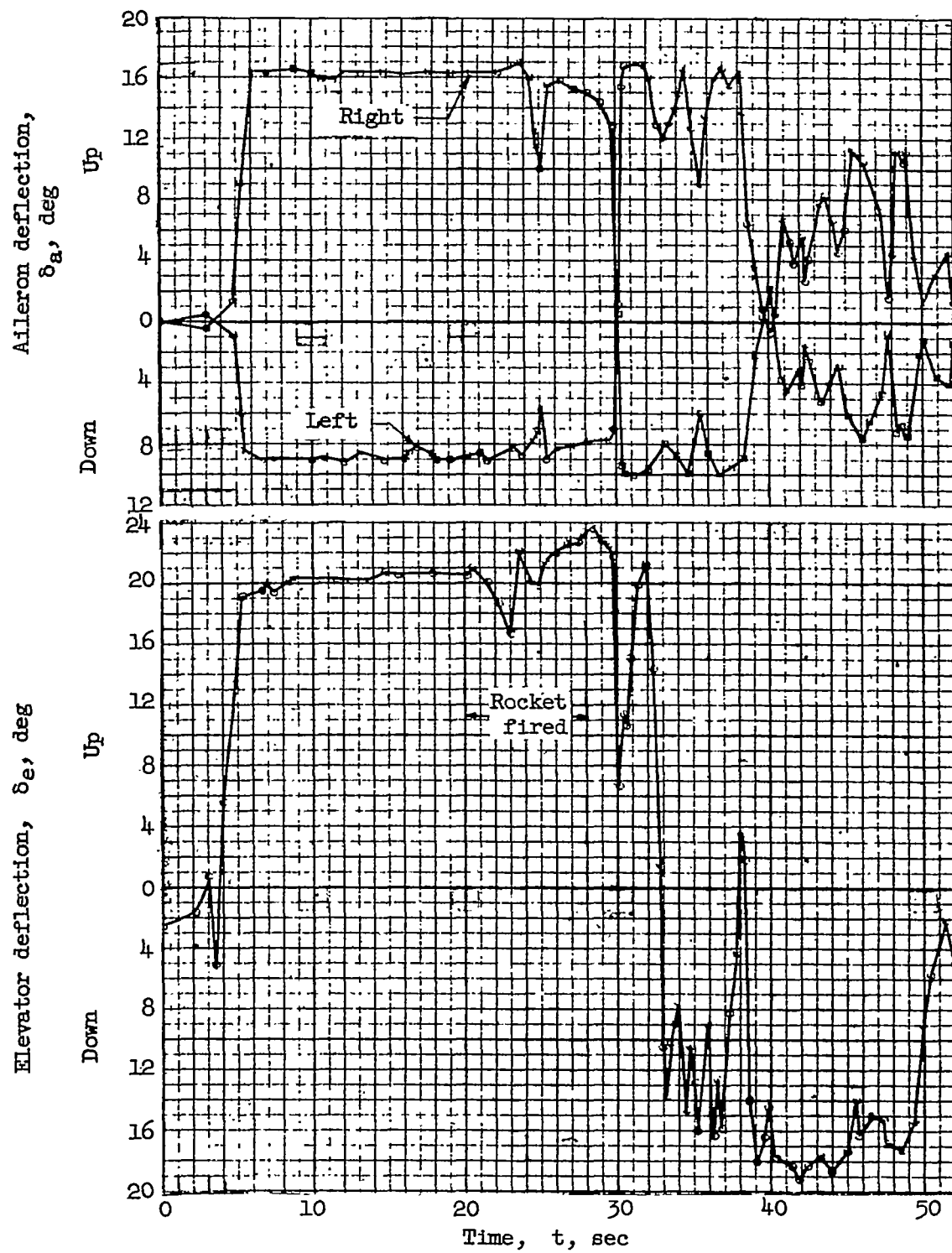
(c)

Figure 13.- Continued.



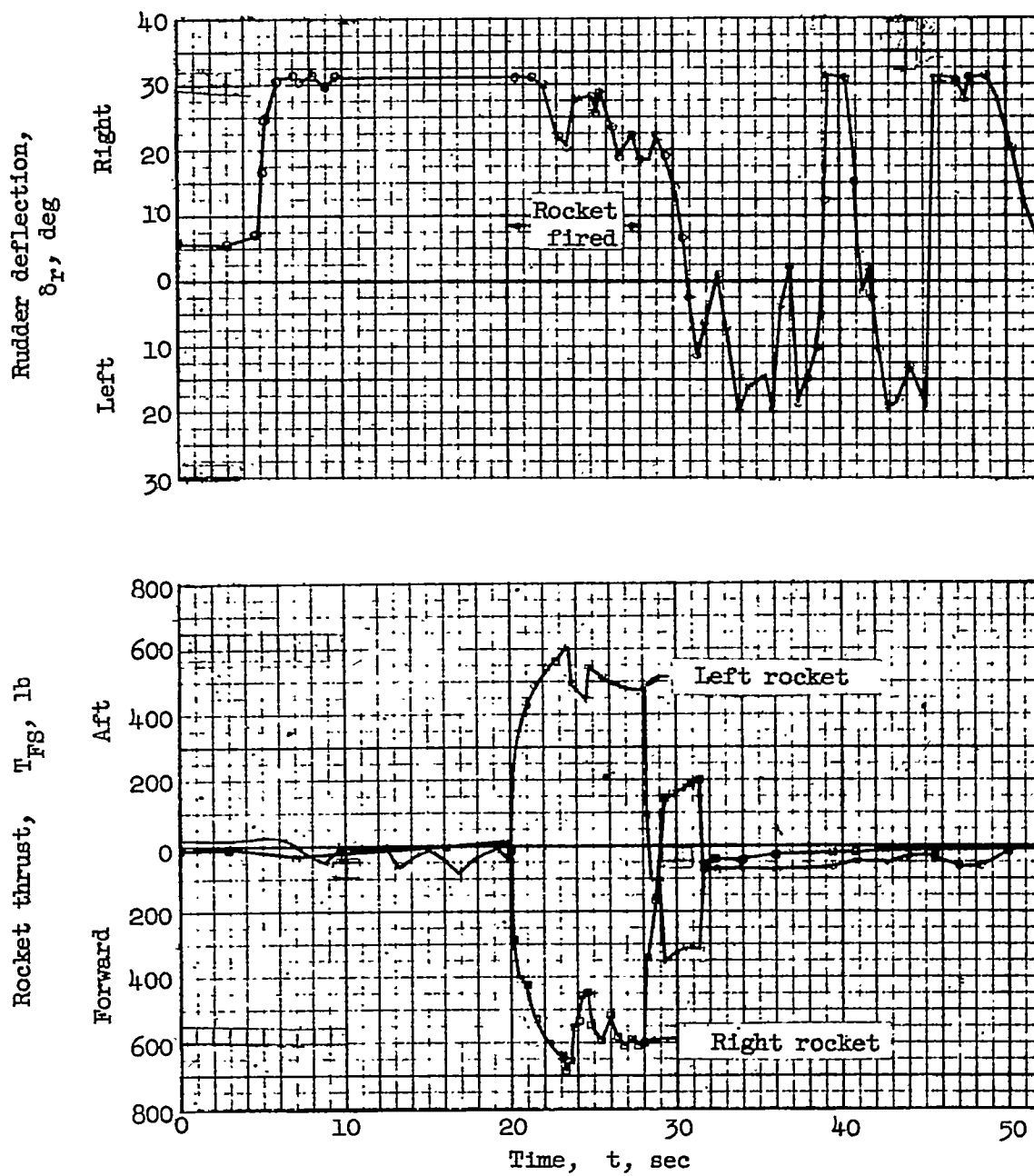
(d)

Figure 13.- Continued.



(e)

Figure 13.- Continued.



(f)

Figure 13.- Concluded.

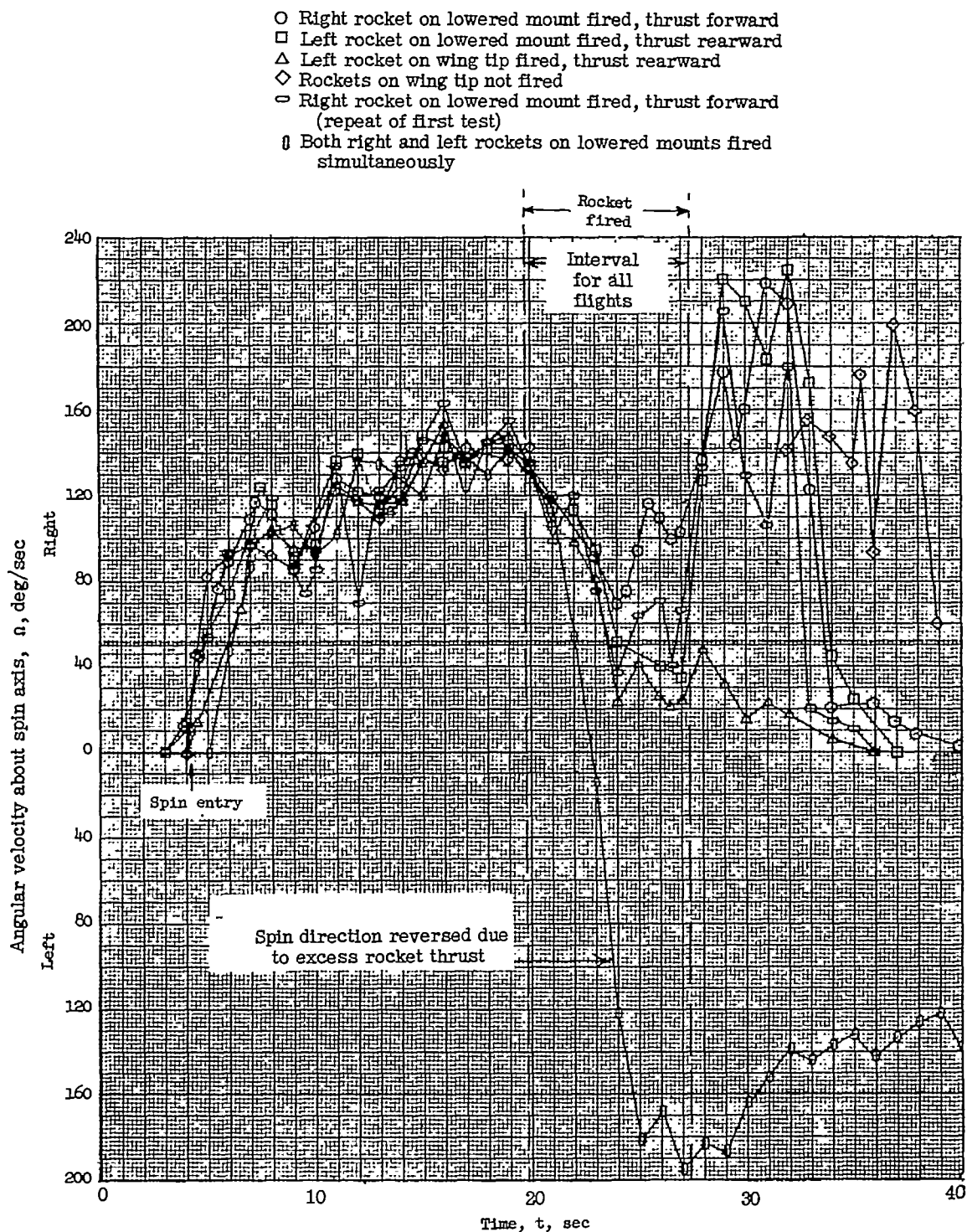
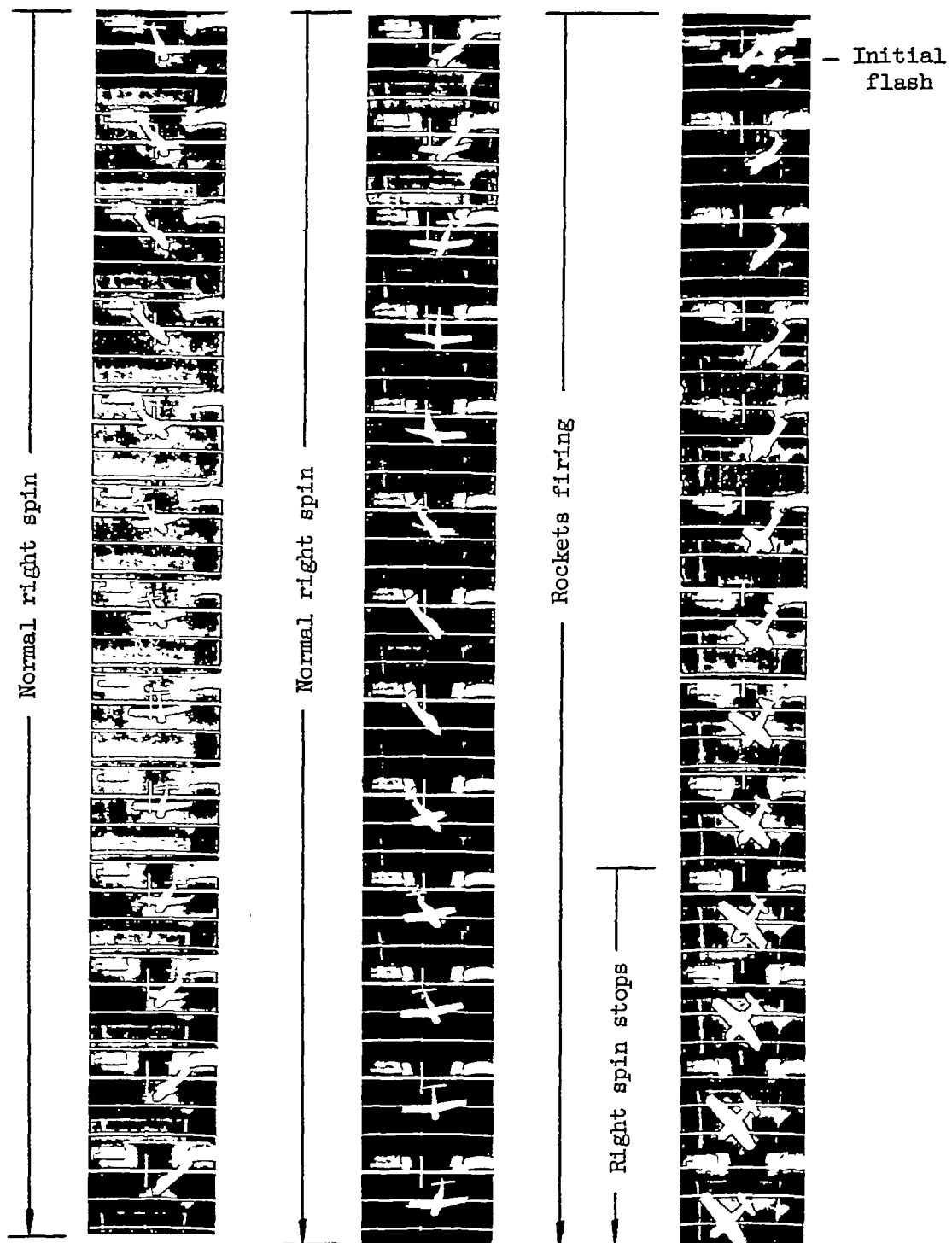
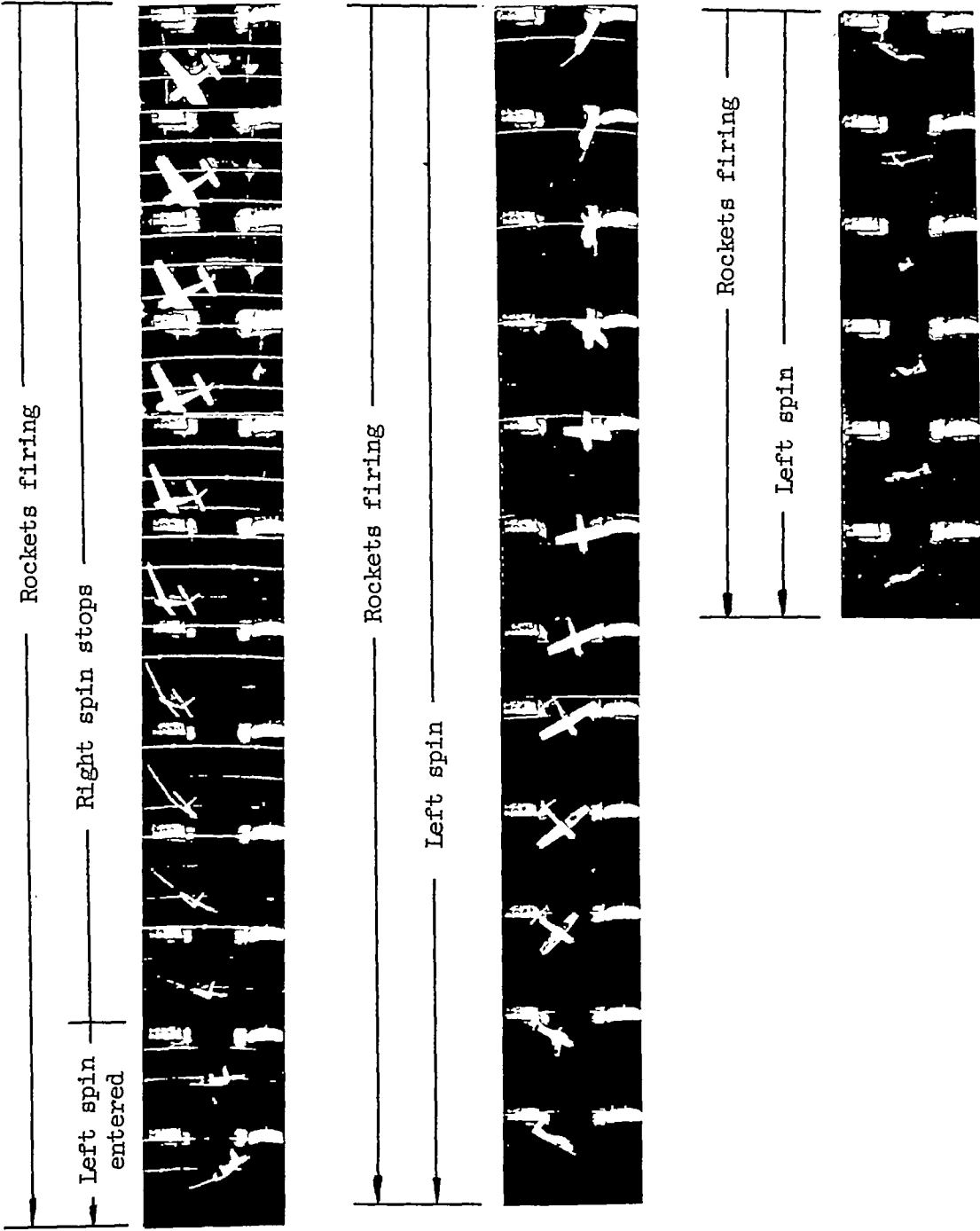


Figure 14.- Time histories of the angular velocities of the airplane about the spin axis for all airplane flights. The rocket firing intervals for each flight have been superimposed on each other. Plots reproduced from reference 3.



L-81279

Figure 15.- Sequence photographs of a model recovery from a right spin by use of both right- and left-wing-tip rockets fired simultaneously. Film speed, 64 frames per second.



L-81280

Figure 15.- Concluded.